US 20130048506A1

(19) **United States**

(12) **Patent Application Publication**

Chen

(10) **Pub. No.: US 2013/0048506 A1**

(43) **Pub. Date: Feb. 28, 2013**

(54) **POROUS METAL DENDRITES AS GAS DIFFUSION ELECTRODES FOR HIGH EFFICIENCY AQUEOUS REDUCTION OF CO2 TO HYDROCARBONS**

(71) Applicant: **The Trustees of Columbia University in the City of**, New York, NY (US)

(72) Inventor: **Ed Chen**, New York, NY (US)

(73) Assignee: **The Trustees of Columbia University in the City of New York**, New York, NY (US)

(21) Appl. No.: **13/659,354**

(22) Filed: **Oct. 24, 2012**

Related U.S. Application Data

(63) Continuation of application No. PCT/US2011/038601, filed on May 31, 2011.

(60) Provisional application No. 61/349,744, filed on May 28, 2010.

Publication Classification

(51) **Int. Cl.**

C25B 15/08	(2006.01)
C25B 3/00	(2006.01)
C25D 9/02	(2006.01)
C25B 11/03	(2006.01)

(52) **U.S. Cl.** **205/317**; 204/242; 204/233; 204/275.1; 204/277; 204/284; 205/462

(57) **ABSTRACT**

An electrolytic cell system to convert carbon dioxide to a hydrocarbon that includes a first electrode including a substrate having a metal porous dendritic structure applied thereon; a second electrode, and an electrical input adapted for coupling to a source of electricity, for applying a voltage across the first electrode and the second electrode.

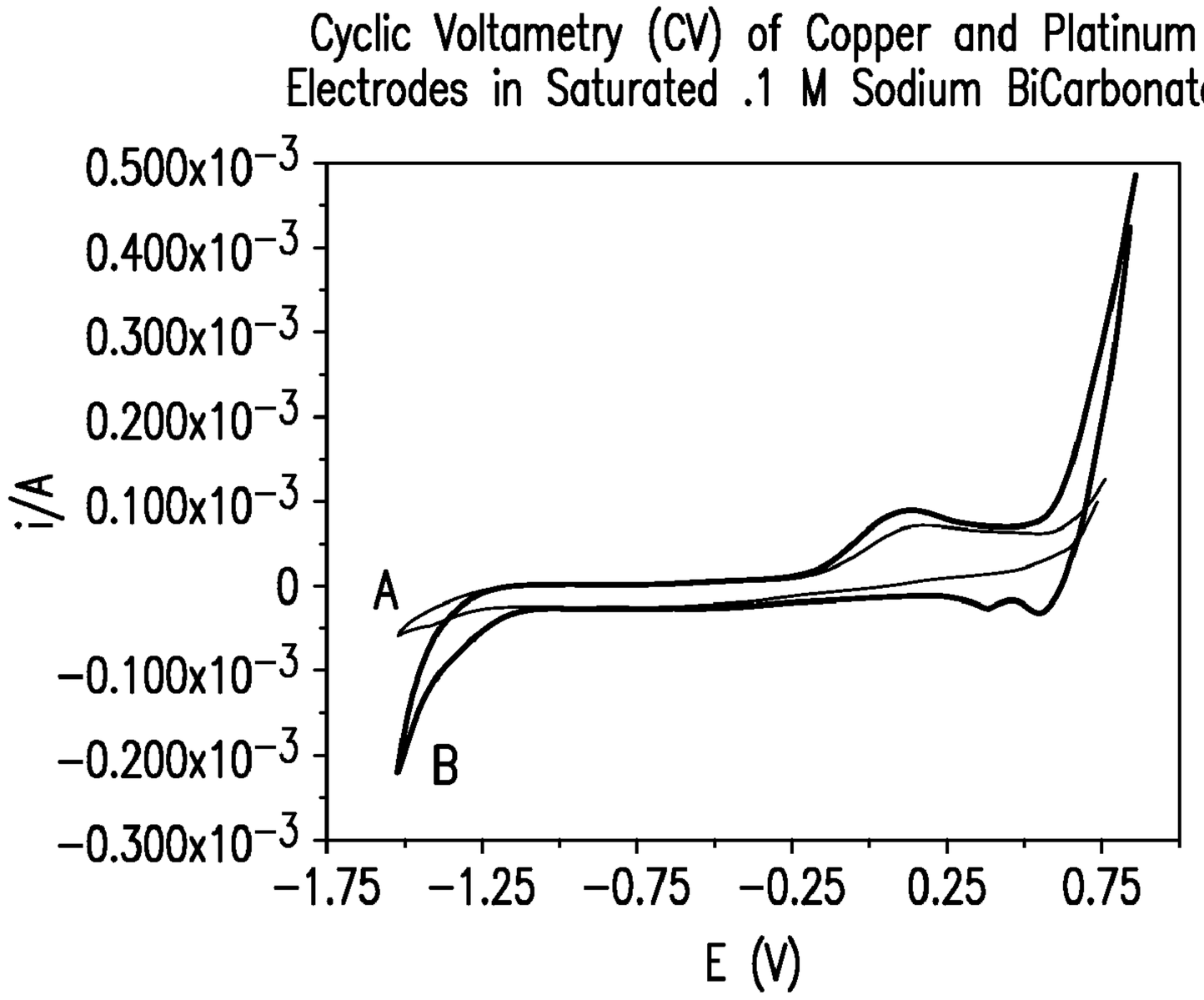
Cyclic Voltametry (CV) of Copper and Platinum
Electrodes in Saturated .1 M Sodium BiCarbonate
0.500x10−3
0.400x10−3
0.300x10−3
0.200x10−3
0.100x10−3
0
−0.100x10−3
−0.200x10−3
−0.300x10−3
i/A
A
B
−1.75
−1.25
−0.75
−0.25
0.25
0.75
E (V)

FIG. 1

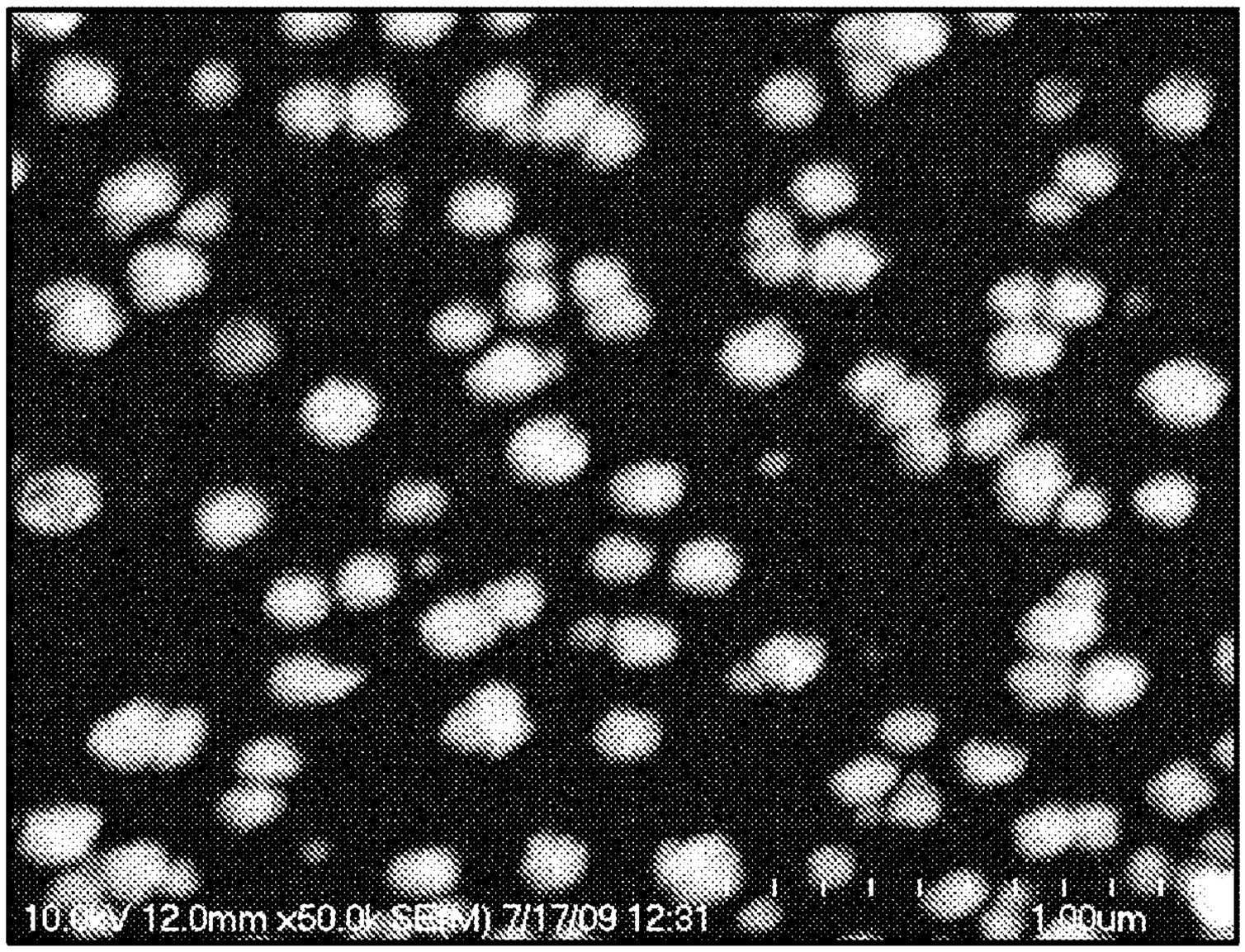

FIG. 2

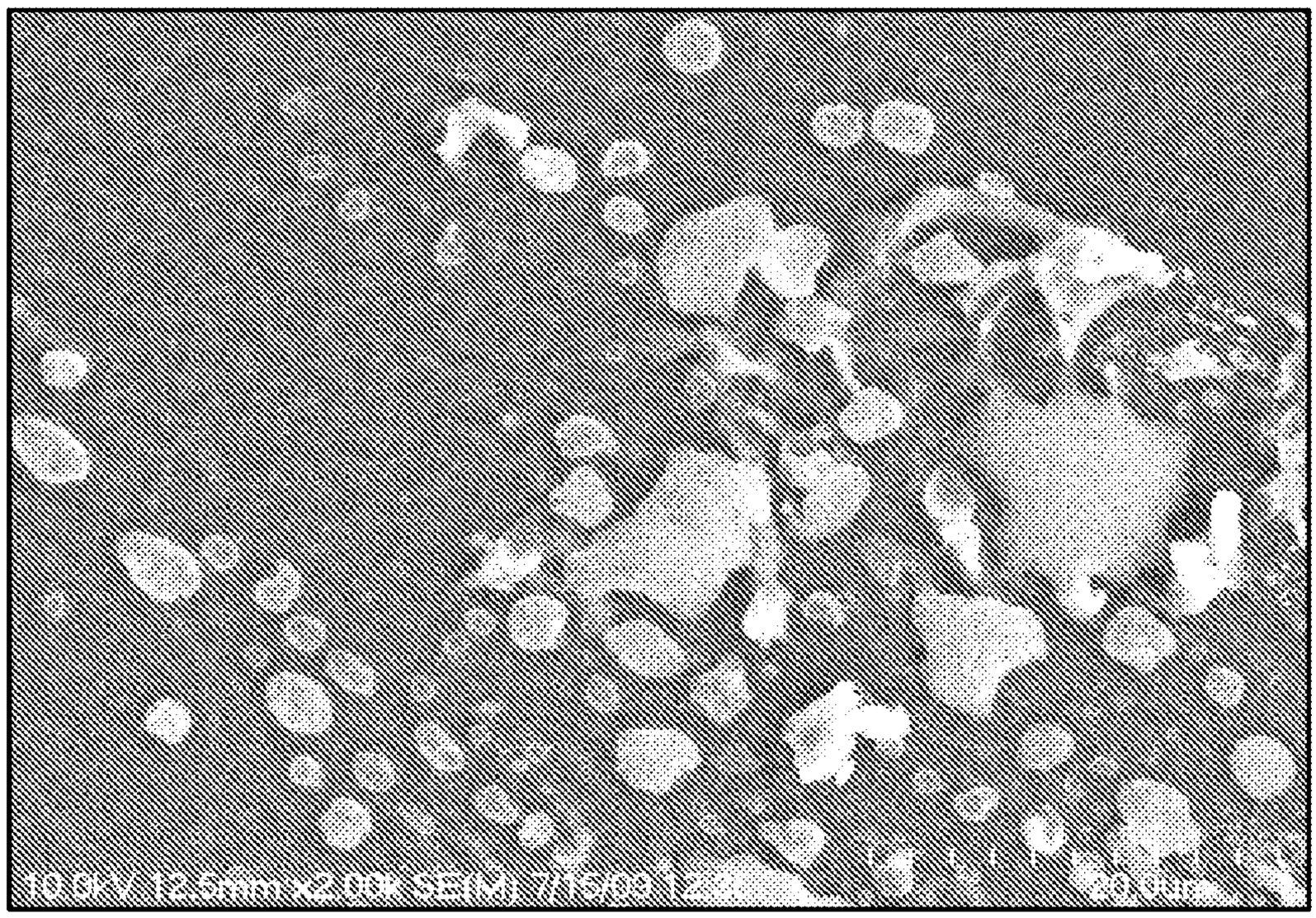

FIG. 3

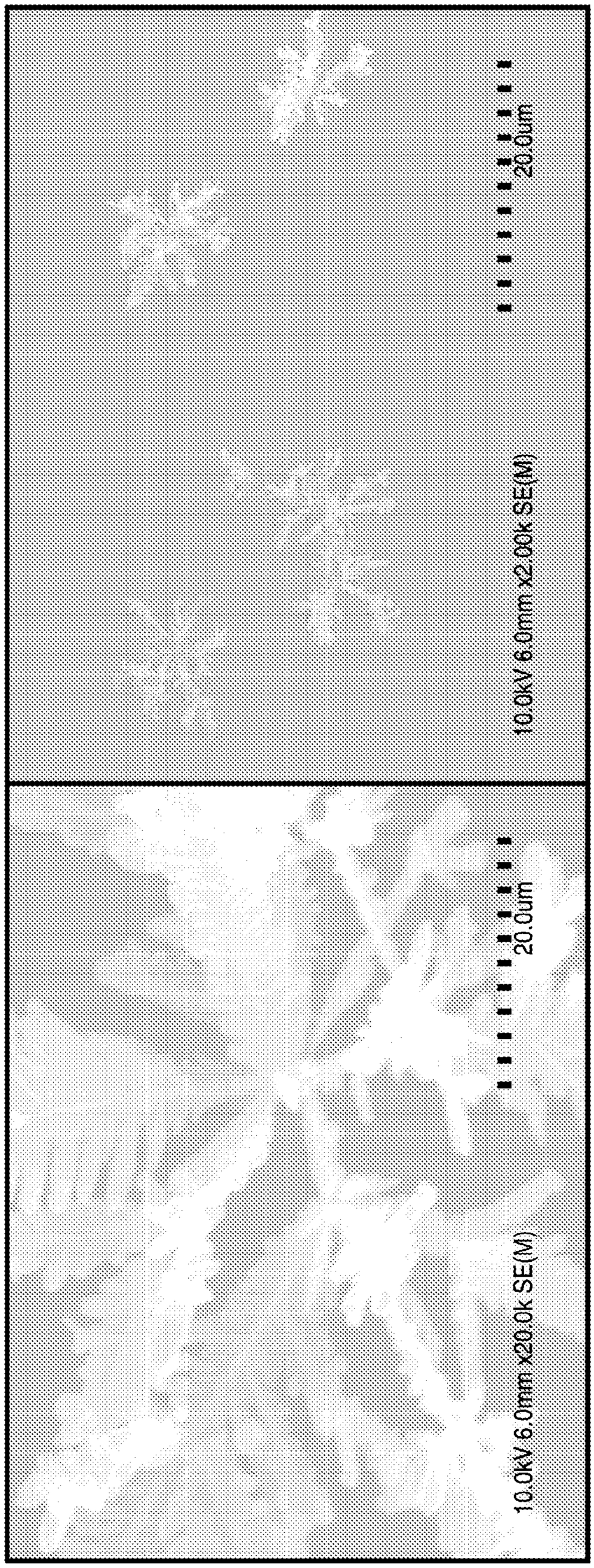

FIG. 4

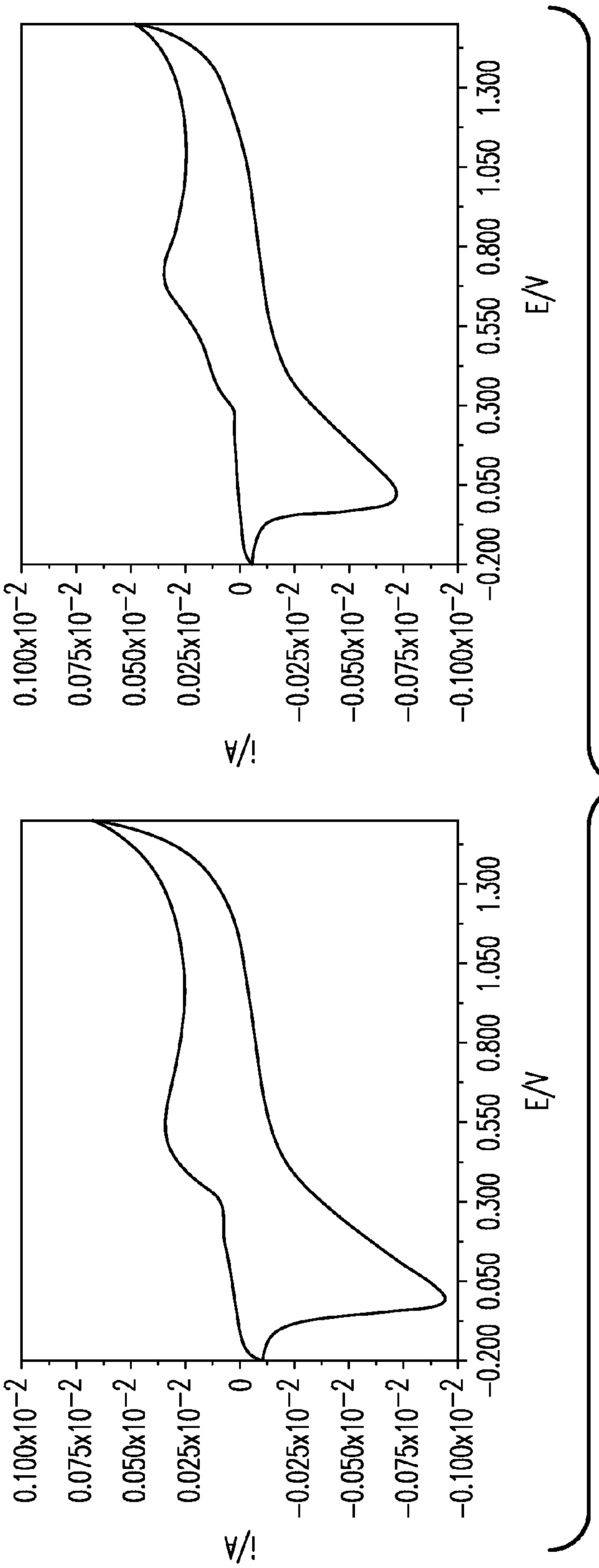
i/A
0.100x10−2
0.075x10−2
0.050x10−2
0.025x10−2
0
−0.025x10−2
−0.050x10−2
−0.075x10−2
−0.100x10−2
−0.200
0.050
0.300
0.550
0.800
1.050
1.300
E/V

FIG. 5

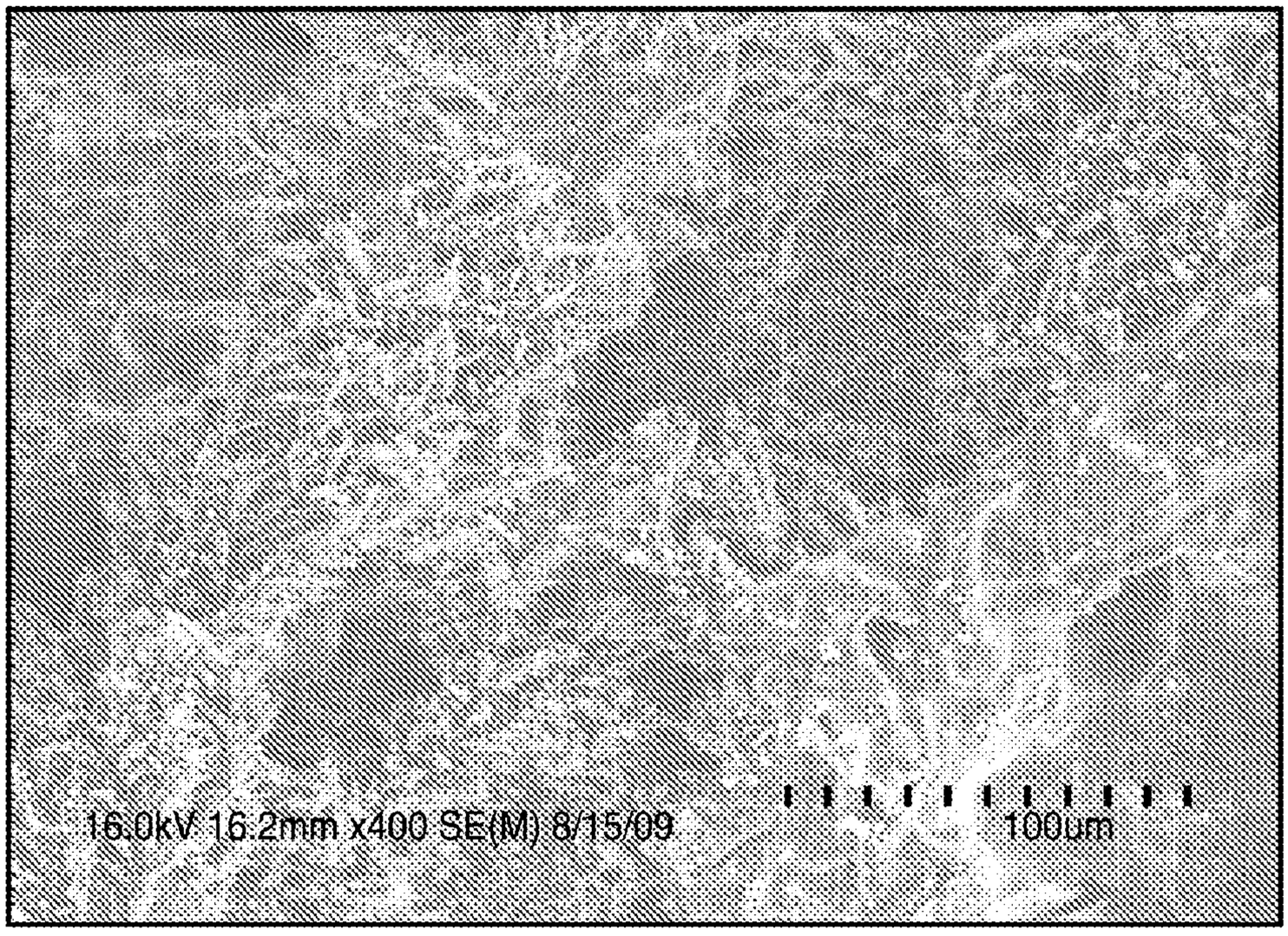

FIG. 6

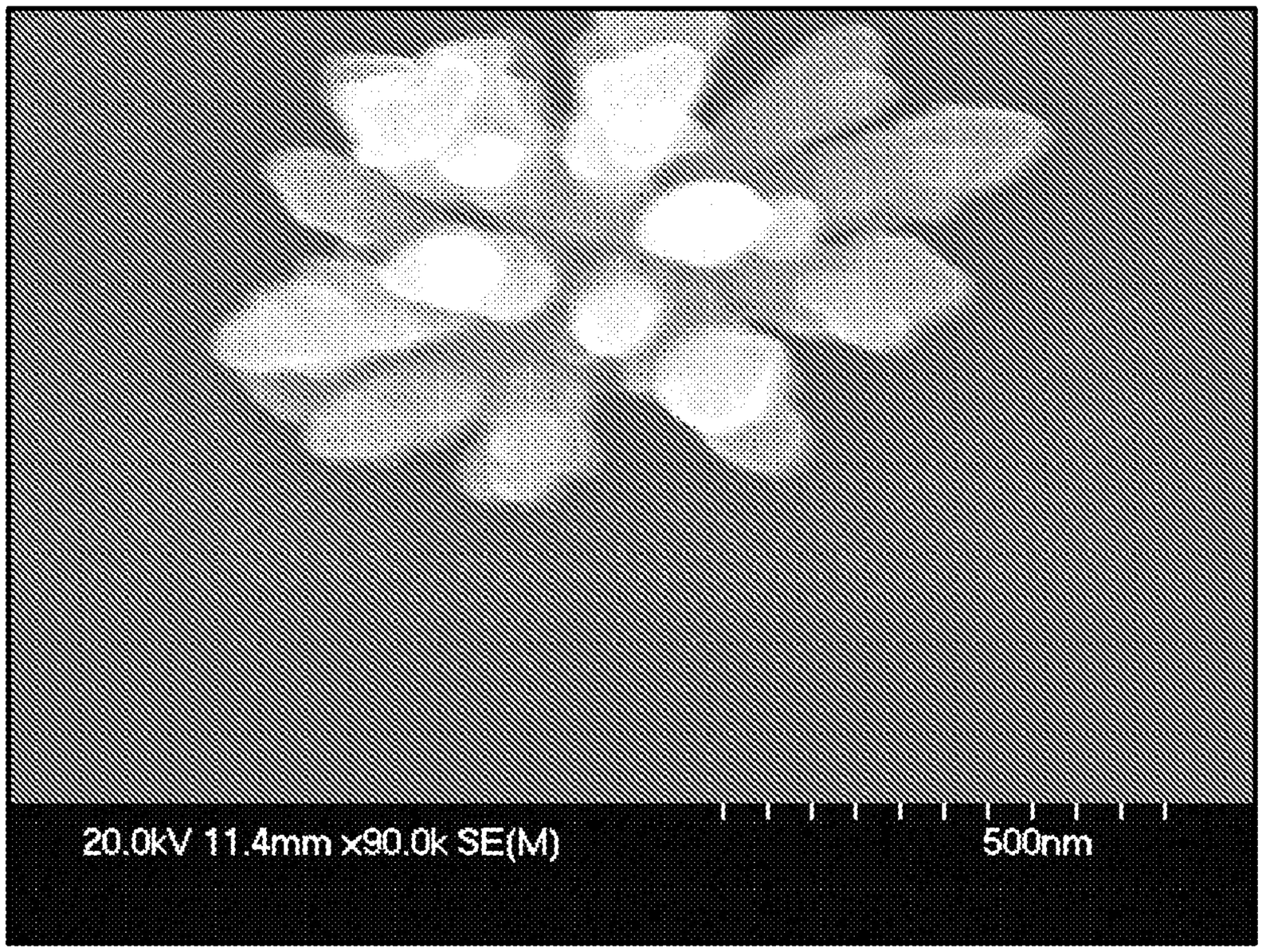

FIG. 7

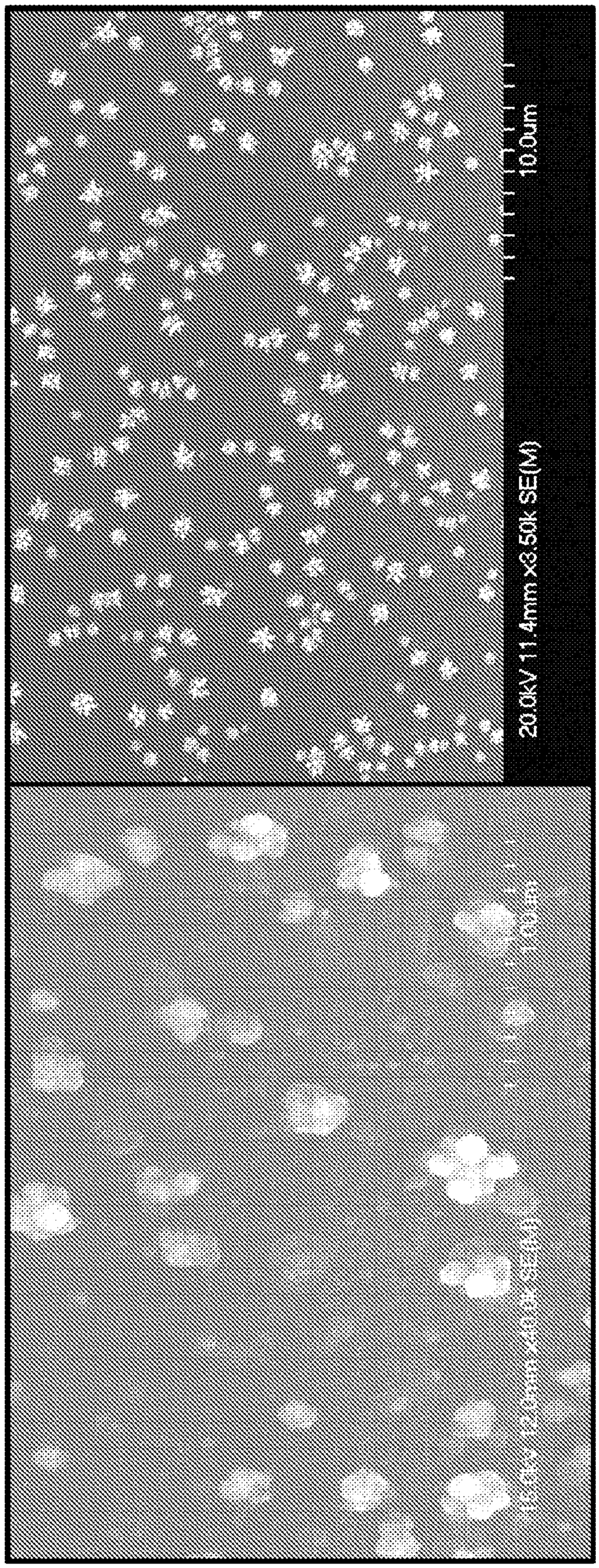

FIG. 8

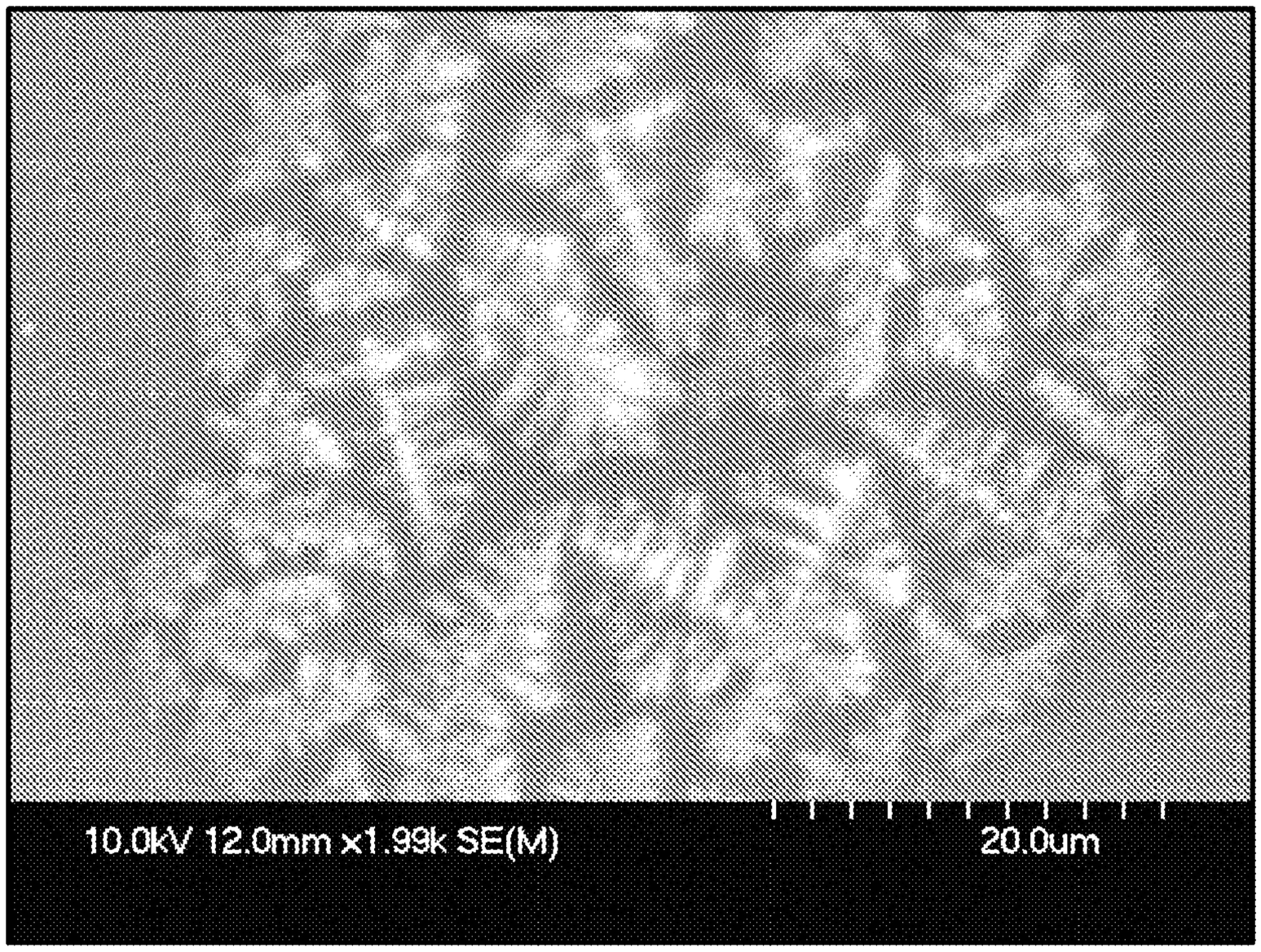

FIG. 9

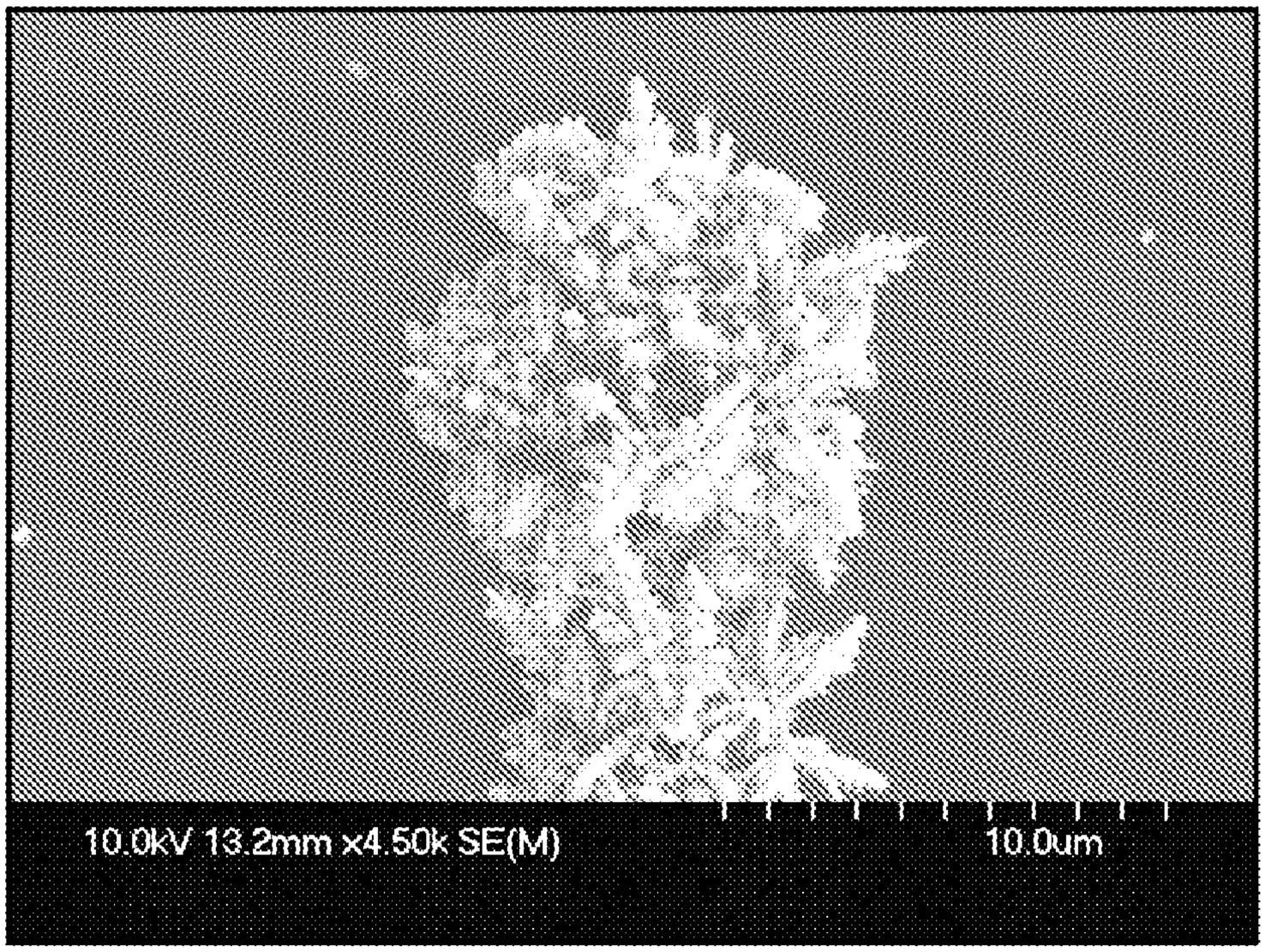

FIG. 10

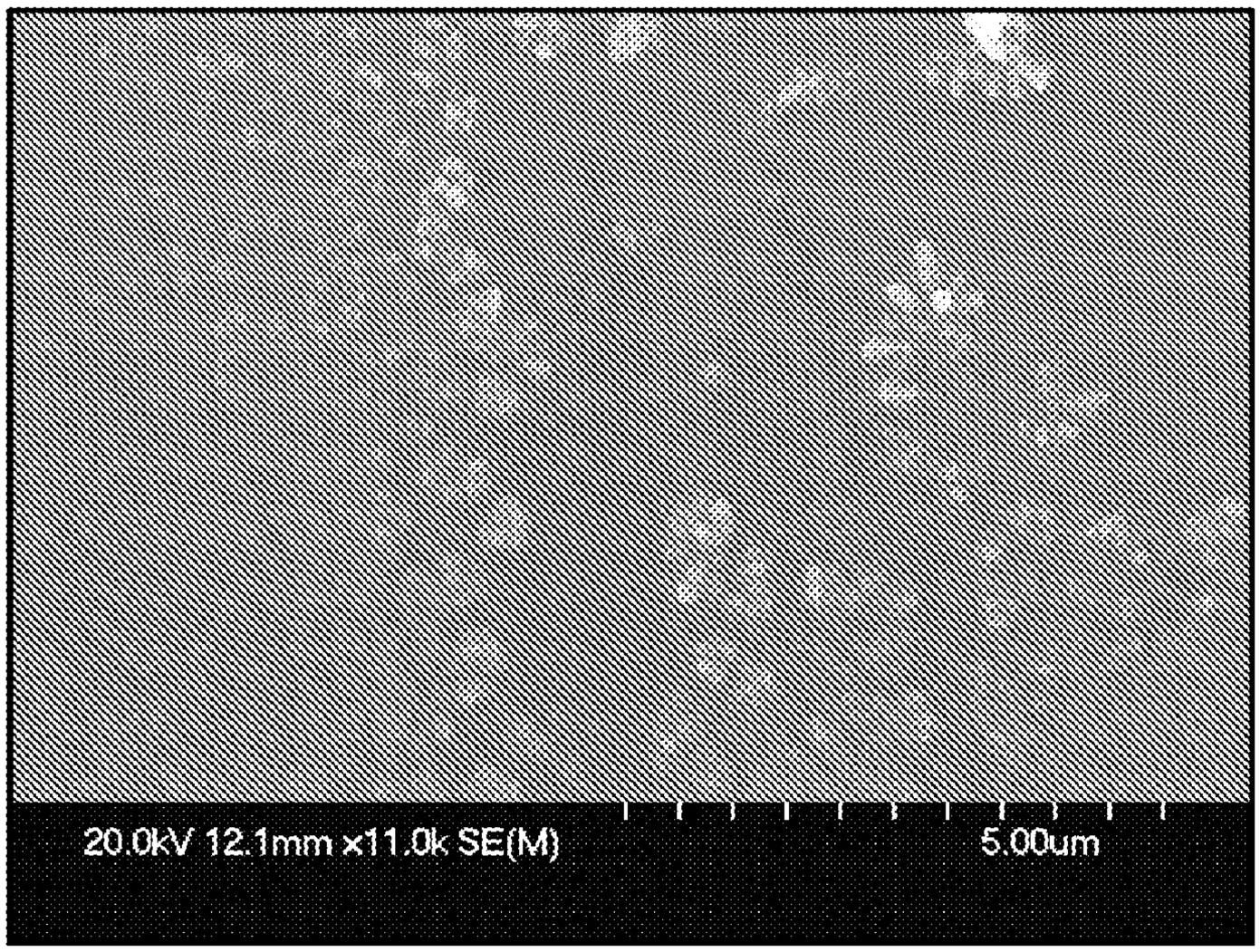

FIG. 11

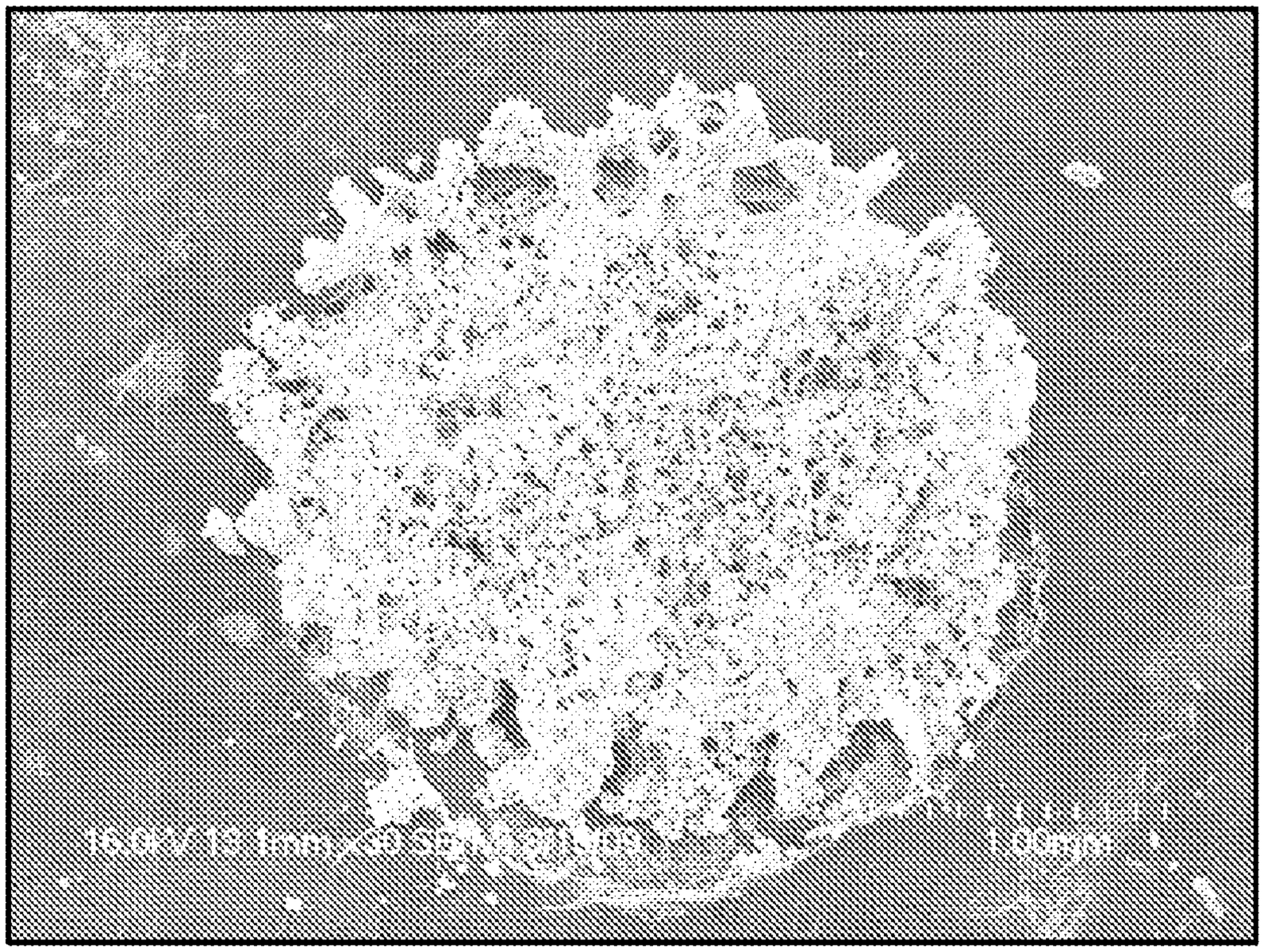

FIG. 12

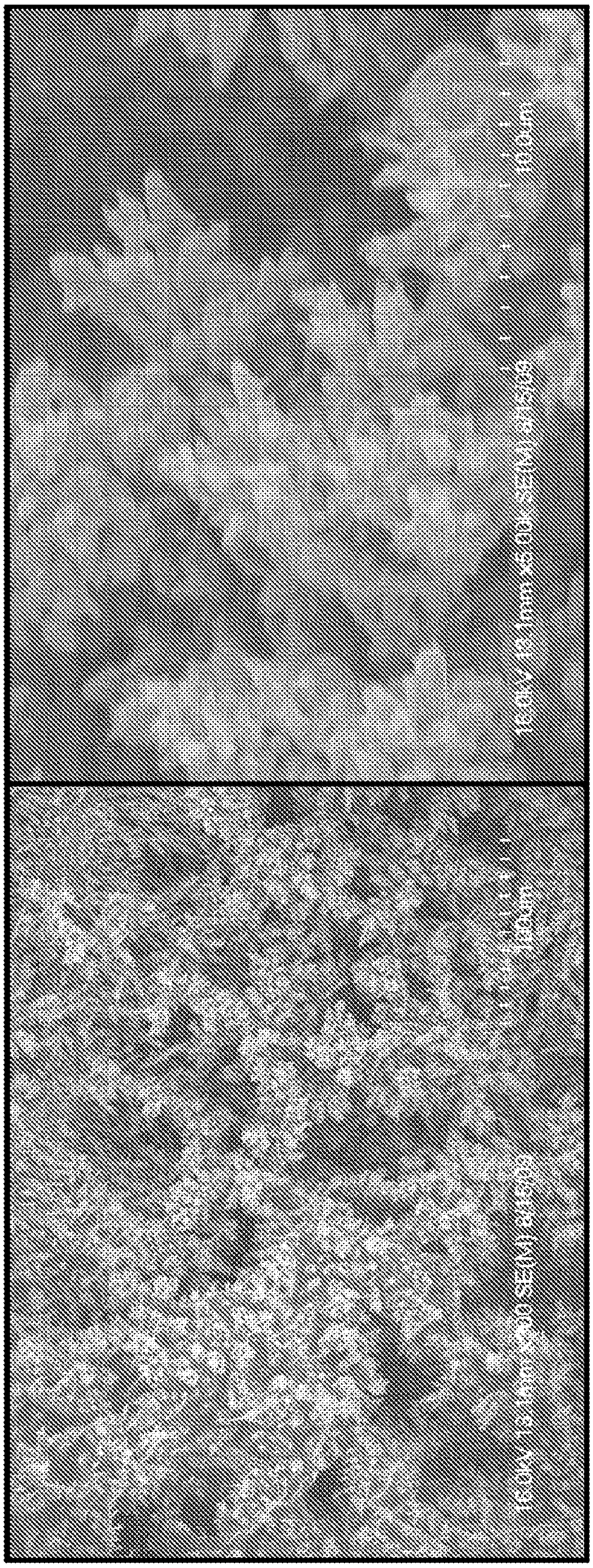

FIG. 13

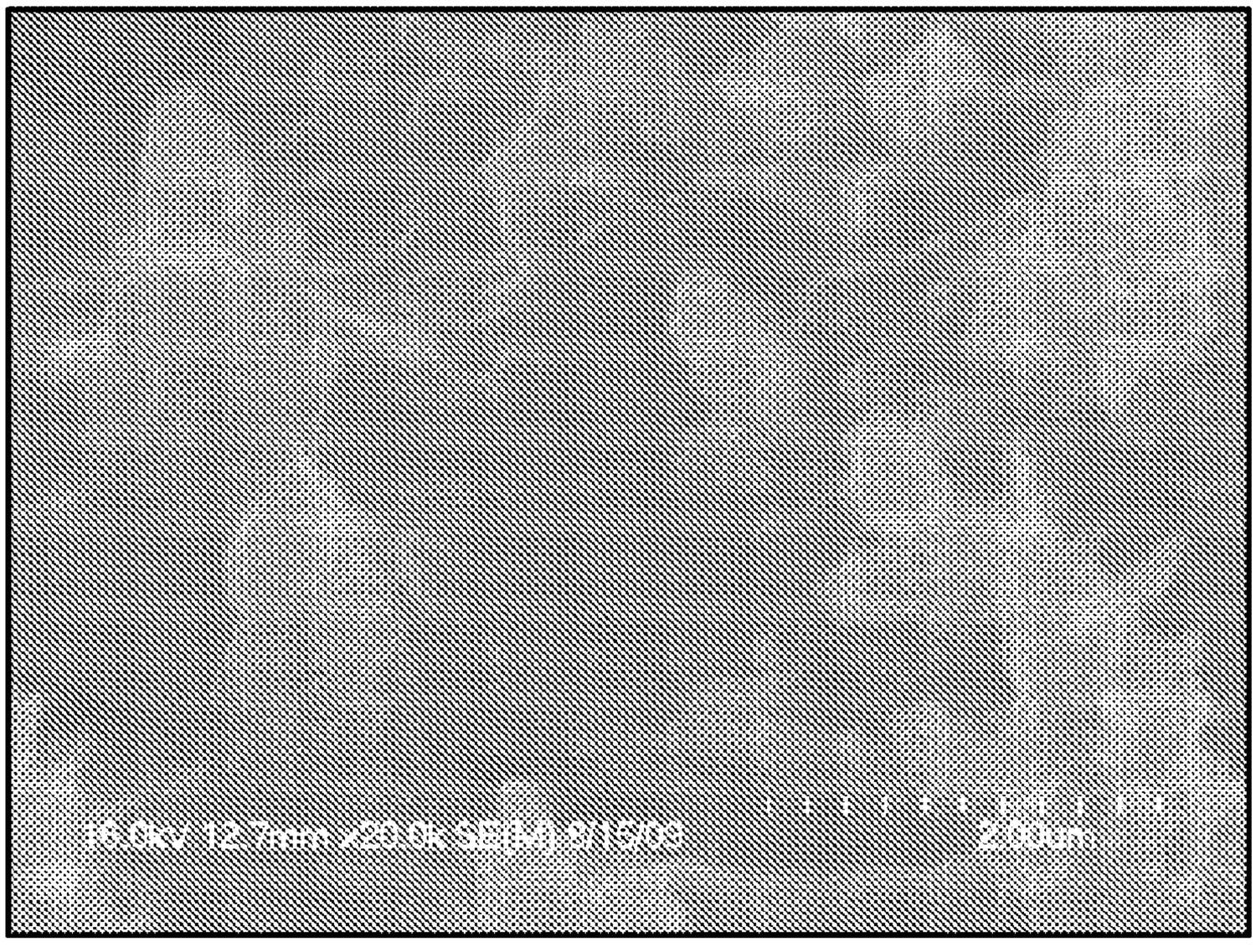

FIG. 14

POROUS METAL DENDRITES AS GAS DIFFUSION ELECTRODES FOR HIGH EFFICIENCY AQUEOUS REDUCTION OF CO2 TO HYDROCARBONS

CROSS REFERENCE TO RELATED APPLICATIONS

[0001] This application is a continuation of International Patent Application Serial No. PCT/US2011/038601 filed May 31, 2011, which claims priority to U.S. Provisional Application Ser. No. 61/349,744, filed May 28, 2010, the contents of both of which are hereby incorporated by reference in their entireties herein.

BACKGROUND

[0002] Existing carbon infrastructure costs make a transition from a fossil fuel economy particularly difficult. Thus, intermediate solutions which abate CO_2 emissions while also producing valuable products would be particularly useful. The use of electrolytic cells in the reduction of CO_2 to methane and other hydrocarbons, electrolytically, at room temperatures, with a saturated solution of carbon dioxide and an electrolyte, can be a highly economic means of producing natural gas from carbon dioxide.

SUMMARY

[0003] One aspect of the presently disclosed subject matter provides an electrolytic cell system to convert carbon dioxide to a hydrocarbon (e.g., ethylene) that includes a first electrode including a substrate having a metal porous dendritic structure applied thereon; a second electrode, and an electrical input adapted for coupling to a source of electricity, for applying a voltage across the first electrode and the second electrode.

[0004] In one embodiment, the metal porous dentritic structure is a metal selected from platinum, gold, silver, zinc, cobalt, nickel, tin, palladium and copper. In one embodiment, the metal porous dendritic structure is a copper dendritic structure. In one embodiment, the substrate is selected from copper, copper foil, glassy carbon and titanium. The first electrode and/or the second electrode can be at least partially saturated with carbon dioxide.

[0005] The presently disclosed electrolytic cell system can further include an electrolyte source capable of being introduced into a region in between the first electrode and the second electrode of the electrolytic cell system. In one embodiment, the electrolyte is selected from a bicarbonate salt (e.g., potassium hydrogen carbonate), sodium chloride, carbonic acid, hydrogen, potassium and methanol.

[0006] In one embodiment, the electrolytic cell system can include a membrane to dissolve carbon dioxide in the electrolyte. In an alternative embodiment, the electrolytic cell system includes a conduit to pass carbon dioxide directly to the surface of the first electrode.

[0007] The presently disclosed electrolytic cell system can further include a source of a metal porphryrin salt capable of being introduced into a region in between the first electrode and the second electrode of the electrolytic cell system. For example, the metal porphyrin salt can be a metal chlorophyllin salt, such as copper chlorophyllin.

[0008] Another aspect of the presently disclosed subject matter provides an electrode for an electrolytic cell system comprising a substrate with a metal porous dendritic structure applied thereon. The metal can be selected from platinum, gold, silver, zinc, cobalt, nickel, tin, palladium and copper.

[0009] Another aspect of the presently disclosed subject matter provides a method of converting carbon dioxide to a hydrocarbon (e.g., ethylene) that includes providing an electrolytic cell that includes a first electrode including a substrate having a metal porous dendritic structure applied thereon; a second electrode, and an electrical input adapted for coupling to a source of electricity, for applying a voltage across the first electrode and the second electrode; introducing a source of carbon dioxide to the electrolytic cell; and applying the voltage across the first electrode and the second electrode.

[0010] The metal of the pourous dendritic structure can be selected from platinum, gold, silver, zinc, cobalt, nickel, tin, palladium and copper. The copper dendritic structure can be prepared, for example, by a process that includes adding copper chlorophyllin to the electrolytic cell and electrodepositing the copper chlorophyllin on the first electrode.

[0011] In one embodiment, the carbon dioxide is obtained from an air stream, a combustion exhaust stream, or a pre-existing carbon dioxide source.

[0012] Another aspect of the presently disclosed subject matter provides a method for preparing an electrode for use in an electrolytic cell that includes providing an electrolytic cell; applying a solution of a metal porphyrin salt to the electrolytic cell; and applying electricity to plate the metal porphyrin salt on the substrate. The metal porphyrin salt can be a metal chlorophyllin salt (e.g., copper chlorophyllin).

[0013] In one embodiment, the metal porphyrin salt is pulse plated or reverse pulse plated on the substrate. According to an alternative embodiment, the metal porphyrin salt is applied to the substrate using high current density to create hydrogen bubble templates on the surface of the substrate.

BRIEF DESCRIPTION OF THE DRAWINGS

[0014] FIG. **1** depicts a cyclic voltametry (CV) of copper and platinum electrodes immersed in a 0.1 M sodium bicarbonate solution saturated with carbon dioxide. The A) red line graph is a CV of a piece of copper foil 0.2 grams in mass, while B) the blue line is a CV of porous copper dendritic electrode with a mass of 5 mg. Current densities for the porous copper is much higher, despite the differences in mass. As reproduced in black and white, the "red" line (A) are the two lines that have the highest i/A at about −1.5 volts and the "blue lines" (B) are the two lines that have the lowest i/A at about −1.5 volts.

[0015] FIG. **2** is a photograph of copper deposits grown at 150 mA/cm^2 with PVA.

[0016] FIG. **3** is a photograph of copper deposits grown at 150 mA/cm^2 with no additive.

[0017] FIG. **4** is a photograph of copper grown with a PEG additive on glassy carbon.

[0018] FIG. **5** is a cyclic voltametry (CV) a high acid copper solution 10 g/L Cu, and 32 g/L of sulfuric acid (left diagram) and CV of high acid copper solution 10 g/L Cu and 32 g/L sulfuric acid with 1% chlorophyllin additive.

[0019] FIG. **6** is a photograph of chlorophllyn residue on porous structure during reverse pulse application, magnified 400 times. The chlorophllyn membrane is attracted to the anode, and is selectively pulled off of the growing fractal front while remaining in the recessed regions, containing loss of surface area while increasing growth of surface area.

[0020] FIG. **7** is a photograph of copper particles formed with chlorophyllin additive and 10 alternating pulses of −0.32

A/cm^2 and 0.1 A/cm^2. Copper structures can be resolved down to 50 nm, and take on a non-spherical form which display higher surface areas.

[0021] FIG. **8** is a photograph of copper particles formed with chlorophyllin additive and 10 alternating pulses of −0.32 A/cm^2 and 0.1 A/cm^2. Copper structures can be resolved down to 50 nm, and take on a non-spherical form which provide higher surface areas.

[0022] FIG. **9** is a photograph of a dendritic fractal cluster produced under a pulsating regime of 500 pulses with a current density of 0.69 A/cm^2.

[0023] FIG. **10** is a photograph of a dendritic structure after a pulsating regime of 1000 pulses with a current density of 0.69 A/cm^2.

[0024] FIG. **11** is a photograph showing the beginnings of the dendritic copper foam beginning to form.

[0025] FIG. **12** is a photograph of copper PDS for visual characterization magnified 30 times.

[0026] FIG. **13** is a photograph of copper PDS magnified 300 times and 5000 times.

[0027] FIG. **14** is a photograph of a dendrite structure magnified 20,000 times.

DETAILED DESCRIPTION

[0028] The presently disclosed subject matter provides a method of converting CO_2 to methanol, methane and other hydrocarbons in an electrolytic cell. In one embodiment, the method includes introducing an electrolyte saturated with CO_2 to an electrolytic cell that includes a substrate with a metal plated thereon, and applying electricity to the electrolytic cell to electrochemically reduce the CO_2. The metal can be selected from, for example, Pt, Au, Ag, Zn, Co, Pb, Ni, Pd and Cu. In one embodiment the substrate is plated with a metal porous dendritic structure, such as a copper porous dendritic structure. Substrates can include, but are not limited to, glassy carbon and titanium. Electrolytes can include, but are not limited to, sodium chloride, sodium carbonate, sodium bicarbonate and potassium hydrogen carbonate.

[0029] The presently disclosed subject matter also provides an electrolytic cell system that includes an electrolyte saturated with carbon dioxide, a cathode that includes a substrate with a metal plating, and a source of electricity capable of being applied to the electrolytic cell. The metal can be selected from, for example, Pt, Au, Ag, Zn, Co, Ni and Cu. In one embodiment the substrate is plated with a metal porous dendritic structure, such as a a copper porous dendritic structure. Substrates can include, but are not limited to, glassy carbon and titanium.

[0030] In one embodiment, a metal porous dendritic structure is obtained using a metal porphyrin salt. As used herein, "porphyrin" refers to a cyclic structure composed of four pyrrole rings together with four nitrogen atoms and two replaceable hydrogens for which various metal atoms can readily be substituted. Porphyrins may be substituted or unsubstituted. An example of a porphyrin is chlorophyllin. Porphyrins, many of which are naturally-occurring, can be obtained from commercial sources. Alternatively, porphyrins can be synthesized. See, e.g., P. Rothemund (1936): "A New Porphyrin Synthesis. The Synthesis of Porphin," J. Am. Chem. Soc. 58 (4): 625-627; P. Rothemund (1935): "Formation of Porphyrins from Pyrrole and Aldehydes". J. Am. Chem. Soc. 57 (10): 2010-2011, each of which hereby incorporated by reference.

[0031] In one embodiment of the presently disclosed subject matter, an electrode is prepared by pulse and reverse pulse plating a substrate with a copper porous dendritic structure using a copper chlorophyllin salt as one of the copper sources. This electrode can be used in the methods and systems described herein.

[0032] Metal Porous Dendritic Structures (PDS) (e.g., Copper Porous Dendritic Structures) can be a high performance material in the catalysis of carbon dioxide as well as air capture and electrolytic reduction of CO_2 due to the high surface areas as well as the absorptive catalytic capacity of Copper PDS. For example, copper PDS can solve one of the major difficulties in the electrolytic reduction of CO_2, as presented in the literature—constructing a electrode which maximizes adsorption of gaseous CO_2 in the reduction reaction with H_2 on the cathode surface. This can allow a commercially feasible process linking electrolytic reduction with air capture, and, in certain embodiments, create a standard temperature and pressure (STP) Fischer Tropsch (FT) device.

[0033] Electrodes can be created using a plating mechanism which has been described. See, e.g., Nikolic N D, K I Popov, Lj. J. Pavlovic, M G Pavlovic. "The Effect of Hydrogen Codeposition on the Morphology of Copper Electrodeposits. I. The Concept of Effective Overpotential:" Journal of Electroanalytical Chemistry, 558 (2006) 88-98, which is hereby incorporated by reference.

[0034] According to one non-limiting embodiment, a bath of copper sulfate and sulfuric acid solution (10 g/L Cu, 32 g/L H_2SO_4) can be prepared. An Autolab 4800 Potentiostat can be used with a glassy carbon and copper PDS cathode and a platinum wire anode. Copper Chlorophyllin salt ($C_{34}H_{31}CuN_4O_{6.3}Na$ Sigma Commercial Grade) can be added to the solution at 1% by weight. Because chlorophyllin is characterized by anodic attraction, the reverse pulse regime creates regions of chlorophyllin membranes covering the dendritic structures, creating additional diffusion-limited growth of dendrites of a smaller scale. Pulse and reverse pulse electrodeposition can be used to form microporous, copper PDS (SEM photos included). A current density of pulsating regimes of −0.015 and 0.01 can be used, which translates into a current density of −0.32 A/m^2 and 0.21 A/m^2 of 15 ms and 5 ms respectively. This regime can be repeated numerous times (e.g., 10,000 times), which creates a small pore on the glassy carbon. A microporous correl structure results.

[0035] The presently disclosed subject matter provides electrodes grown in this manner, as well as electroless plating of other nobel metals such as, but not limited to, Pt, Au, Ag, as well as other metals such as Zn, Co, Ni to the copper template to electrochemically reduce CO_2 to hydrocarbons (e.g., ethylene) using electricity in an electrolytic cell which can use sodium bicarbonate or potassium bicarbonate as the electrolyte, or methanol. CO_2 can be dissolved into electrolyte using a membrane, such as a liquicell membrane. In certain embodiments, potentials can vary from, for example, −0.5 V to −3 V vs. SHE.

[0036] Emobidments of the presently disclosed subject matter provides rapid electrochemical reduction of CO_2 to hydrocarbons at current efficiencies of more than, for example, 100 times more than copper foil per gram. Unique products can also be produced on the electrode including C_2 to C_6 hydrocarbons, formate, ethylene, propane, and methanol. In one embodiment, ethylene is the primary hydrocarbon produced by the electrolytic cell system.

[0037] Using the pulse reverse pulse technique along with copper chlorophyllin additive, BET surface areas were measured between 20 to 41 m^2/gram. Use of these electrodes can profitably produce valuable hydrocarbons from carbon dioxide, producing near carbon neutral fuels, while also taking advantage of future and existing carbon credits for offsetting emissions.

[0038] The presently disclosed subject matter provides for the electrolytic reduction of carbon dioxide. Further embodiments provide a process linking electrolytic reduction with air capture, creating a standard temperature and pressure (STP) Fischer Tropsch (FT) device. The mechanics of dendrite formation and review of the theoretical literature on fractal catalyst simulations is also provided.

[0039] Porous dendritic metal foams can be used in electrocatalytic applications, particularly the conversion of CO_2 directly to useful hydrocarbons, such as ethylene. Furthermore, because these catalysts are both produced and applied in an electrochemical environment, any lost catalyst area can be rapidly regenerated in situ. These possible applications extend to porous copper, platinum, and gold structures on reactions such as the electrocatalytic reduction of CO_2 to C_2-C_6 hydrocarbons, methanol, CO, hydrogen, formate, and other organic compounds, with hydrocarbons being produced at large molar percentages and current densities. The high surface area, coupled with the microporous structure creates outsized absorptivity, while the continuous structure of the foam allows for high electrical conductivity. Finally, continuous absorption of product species leads to further conversion of methane to higher hydrocarbons. BET surface characterization and SEM scans show that dendritic structures have higher surface areas than bulk materials as well as non-dendritic powders. Furthermore, the electrocatalytic and catalytic activities are tested using cyclic voltammetry and calculations indicate that copper PDS have nearly a full order of magnitiude higher BET surface area than dendritic powder, and more than 100 times the electrochemical activity on reduction of carbon dioxide to methane and other hydrocarbons than commercial copper foil.

EXAMPLES

[0040] The present application is further described by means of the examples, presented below. The use of such examples is illustrative only and in no way limits the scope and meaning of the invention or of any exemplified term. Likewise, the invention is not limited to any particular preferred embodiments described herein. Indeed, many modifications and variations of the presently disclosed subject matter will be apparent to those skilled in the art upon reading this specification. The invention is therefore to be limited only by the terms of the appended claims along with the full scope of equivalents to which the claims are entitled.

[0041] The experiment is conducted in three portions. The first experiment involved growing porous fractals which maintained their stability and cohesion to the surface of the substrate. The second phase of the experiments were conducted to determine the surface area of the dendritic pores, compared to spherical copper powder, and dendritic copper powder. Finally, the third phase of the experiment involved testing the efficiency of the copper PDS electrode for electrocatalytic effects on the reduction of CO_2 to higher hydrocarbons.

[0042] One purpose of the growth phase of the experiments are to grow fractal surfaces which can be tested for catalytic activity. Initially, only titanium and glassy carbon produced dendritic structures on their surfaces in this particular example. This is due to the low nucleation densities achieved on the surface of these two substrates. Low nucleation densities result in high current densities, which also have correspondingly high electric potentials. Ultimately glassy carbon is used as substrate for experiments because of the low nucleation densities achieved due to the low conductivity of the glassy carbon, as well as the repeatibility of the surface of glassy carbon. Low nucleation densities on the surface of titanium are due to inconstitent oxidation patterns. Finally, glassy carbon is a substrate of choice in the literature when studying copper crystal growth.

[0043] A bath of copper sulfate and sulfuric acid solution (10 g/L Cu, 32 g/L H_2SO_4) is prepared. An Autolab 4800 Potentiostat is used with a glassy carbon with copper PDS cathode and a platinum wire anode. Copper chlorophyllin salt ($C_{34}H_{31}CuN_4O_{6.3}Na$ Sigma Commercial Grade) is added to the solution at 1% by weight. Because chlorophyllin is characterized by anodic attraction, as observed through visual inspection, the reverse pulse regime creates regions of chlorophyllin membranes covering the dendritic structures, creating additional diffusion-limited growth of dendrites of a smaller scale by limiting the exposure of cathodic surface area and concentrating a high current density on the tips of new dendrites while preventing structures previously grown from smoothing out with more copper particles. The surface of dendrites after an anode phase of a pulse is shown below to demonstrate the chlorophyllin anodic attraction. Other additives used in experiments were PVA, PEG, and PVP. Results of nucleation for each can be displayed.

[0044] Pulse and reverse pulse electrodeposition are used to form microporous, copper PDS. A current of pulsating regimes of –0.015 A and 0.01 A are used, which translated into a current density of –0.32 A/m^2. and 0.21 A/m^2 of 15 ms and 5 ms respectively. This regime is repeated 10,000 times, which creates a small pore on the glassy carbon substrate. A microporous carrel structure results. The conceptual advantages of pulse and reverse pulse plating for standard electroplating applications is discussed in a review by Chandrasekar and Pushpavanam (2007). It creates dissolution, and the potential of new nucleations. Other metals such as zinc and iron, which are known to produce dendrites, can also be used as templates for copper and other metal electrodes through electroless plating.

[0045] To measure the surface area of the copper PDS, as well as to provide a comparison with other copper powders and structures, BET surface area measurements were conducted. The theory of BET surface area measurements can be found in Brunauer, S., P. H. Emmett and E. Teller, J. Am. Chem. Soc., 1938, 60, 309. doi:10.1021/ja01269a023, which is hereby incorporated by reference. The substrate is removed carefully from the electrolyte. If too many pulses are used, pores can lose their structural integrity. Too few pulses, and the pores can be too readily oxidized upon contact with air. Pores are rinsed with deionized water to remove residues of sulfuric acid, then acetone is used to remove deionized water and prevent redissolution of copper PDS. The pore is degassed for a period of six hours at 100° C. in a Quantchrome Nova 3000 Surface Area Analyzer under a nitrogen atmosphere to prevent oxidation. When degassed at significantly higher temperatures, the PDS can lose its structure, or can be

oxidized into a hard brown crust. When degassed at lower temperatures, residues can react with copper and can turn the powder into a blue residue.

[0046] Additional dendritic powder, which are dendritic copper grown at high curent densities without a pulsing regime, are collected and analyzed as free copper which did not remain on substrate. Furthermore, commercially available spherical copper powder is also analyzed. After sample is degassed, pores are then measured for BET surface area by scraping dendritic pores from glassy carbon substrate into a sealed vacuum tube which is evacuated to set pressures, and partial vapor pressures measured with a transducer at each pressure point.

[0047] The resulting foam was collected in free form from a tube chamber within the electrolytic cell. This setup is necessary to maintain the high current densities necessary to produce the foam, while also allowing for the flow of copper ions into the cell. Once the tube is filled with copper, the resulting product is washed with deionized water and placed in an argon atmosphere to prevent oxidation of copper powder. A copper correl structure is also grown on a glassy carbon substrate. The BET surface area of the intact coral structure is measured. Cyclic voltametry is performed on the copper electrode on the oxidation of CO_2 to methanol to compare the activity of the fractal catalyst with the activity of a flat geometry deposit.

[0048] In the third section of the experiment, copper PDS grown on glassy carbon substrate is tested as a electrocatalyst for the reduction of carbon dioxide to higher hydrocarbons. A sealed electrolytic cell is constructed isolating the anode from the cathode so that samples of gas produced could be collected.

[0049] A 0.1 M Na_2CO_3 is prepared with deionized water, and saturated with carbon dioxide by bubbling gas through solution for one hour. A piece of commercially available, thin copper foil (Alfa Aesar Cu foil Puratronic, 99.9999% (metal basis), 0.25 mm thick) is used as an electrode in the reduction process. A MetroOhm Autolab 4800 potentiostat is used, and a platinum wire counterelectrode is used as well. Gas phase products are analyzed using gas chromotography. A volume of 100 ml is extracted from the cell after running the cell for 10 minutes to purge all air from the system. The production of hydrogen and CO is not detected by the GC. Its weight is determined to be 0.2 grams, which is approximately 40 times the weight of the copper dendritic electrode, which had a weight of 0.00503 grams. However, it's apparent surface area is the same when projected to a two dimensional plane.

[0050] This solution was then used as electrolyte for tests. In the literature, regardless of the electrolyte used, whether it was $KHCO_3$, Na_2CO_3, or simply salt, the resulting products did not change (Shibata et al 2008). A copper foil sheet was prepared to have roughly the same surface area as the substrate of glassy carbon. A cyclic voltametry was conducted to determine the difference in activities between the copper foil electrode and the copper PDS electrode. Gas was collected from the sealed cathodic chamber and removed with a syringe. The resulting gases were analyzed using an Agilent Gas Chromatography to confirm the production of methane and ethylene. Furthermore, visual inspect found that there was an oil slick on the surface of the water, though this substance was not analyzed.

Results:

[0051] This results demonstrate that reactions are occurring at the surface of copper fractal catalysts which do not occur on the copper foil catalyst. Furthermore, the results demonstrate that fractal catalysts have a high surface area which also have a high electrical conductance. Finally, it shows that fractal catalysts are two orders of magnitude more efficient per gram than copper foil.

[0052] A copper gas diffusion electrode is fabricated which addresses one of the major needs for improvement—making room temperature and pressure, aqueous electrochemical reduction of carbon dioxide to higher hydrocarbons feasible; this electrode is at least two orders of magnitude more active per gram than an equivalent copper foil. Furthermore, a CV (Cyclic Voltametry) demonstrated that additional reactions occur in the copper PDS electrode as compared to a copper foil electrode, giving some support to the hypothesis that geometrical effect can play a significant role in selectivity of products. A method was found to grow surfaces which are significantly more complex, as measured by BET surface area, than those produced in the literature using techniques which have not yet been reported, namely the addition of chlorophyllin. The interface of the copper surface also can be used as a template for other catalysts, providing the potential for creating unique electrocatalytic alloys.

[0053] Copper PDS electrodes demonstrated electrochemical reduction of CO_2 to hydrocarbons with a peak occurring at a slightly lower potential. Because this process occurs due to adsorption on electrode surfaces, it is possible the gaseous diffusion electrodes would produce higher yields than a simple foil electrode. Copper PDS has very significant surface area and a very low volumetric density. In addition, copper PDS displays many irregularities on its surface, a condition that has been found to be conducive to catalytic reactions, perhaps due to local concentrations in electric field potentials at boundary discontinuities. It is interesting to note that when these structures were placed into the saturated solution of sodium bicarbonate, bubbles nucleated at a far higher rate on the structures, than elsewhere in the solution or other electrodes.

[0054] When the CV is run comparing the copper PDS electrode and a copper foil electrode, an interesting effect is detected. It is immediately apparent that the copper structured into a fractal produced rates of reduction higher than the electrode with a mass almost 40 times greater than the copper dendrite. This is unexpected. The peaks occur at nearly the same places for both the copper foil and the copper foam, though the copper foam displays a slightly lower peak voltage, making the process energetically more efficient. The PDS peak is relatively longer, which can imply there are two competitive processes occurring: the production of methane and perhaps other higher hydrocarbons from hydrogen and carbon dioxide. As the potentials increase, the higher activity of the copper PDS, as compared to the copper foil is apparent. The copper PDS is almost 4 times more efficient, and almost 160 times more efficient per gram.

[0055] Finally, the CV showed another interesting effect for copper PDS gaseous diffusion electrodes. On the negative sweep of the CV, the oxidation peaks for the copper gas diffusion electrode differed from the peaks of the foil electrode. The gas diffusion electrodes showed two peaks, while the foil electrode only showed a single peak. The dual peaks implies that two reverse reactions are occurring, each of a slightly different reaction energy, as shown in FIG. **1**.

[0056] It is interesting that significant production of side reactions occur, and are likely due to the porous structure of the electrode, since the gas reactions only occur when gas is captured on the porous electrode and adsorbed onto the surface of the catalytic metal. Highly dispersed metal particles

are not a better geometry when compared with a porous structure, given the requirements of gaseous adhesion for electrolytic conversion of carbon dioxide to occur. Instead, the unique, fractal geometry of the internal surface of the structure creates a reaction surface, which also traps individual reactant and product gas molecules and confines them within what is essentially a knudsen diffusion regime, though the scalar accuracy of this non-binding proposal can be verified with simulations. The production of ethylene and methane were confirmed with gas chromatography with dendritic copper grown at high current densities.

Results of Experimental Growth of Dendritic Copper:

[0057] The result of the first phase of experiments, which is to grow catalytic fractal surfaces, resulted in SEM scans that showed PVP (FIG. **2**) prevents formation of dendritic nucleations, while no additives, i.e., no PVP, resulted in irregular deposits (FIG. **3**). However, PEG created conditions which allowed for dendritic structures to form on the substrate, though dendrites were much larger than those grown with chlorophyllin (FIG. **4**).

[0058] Copper chlorophyllin is used because of the chelated copper at the center of the molecule, as well as its characteristic anodic attraction during pulsing cycles. SEM photographs are taken of the structures after a short number of pulses, as well as longer pulses. From these photographs, it can be seen that the addition of chlorophyllin resulted in the further branching of the nucleating copper particles. Photographs are given from spherical nucleation of copper obtained without additives, to the nucleation of copper with more structure on smaller scales with chlorophyllin as an additive. Nucleation without additives can be controlled to 100 nm. However, using a chlorophyllin additive, structures can be resolved to 50 nm and particles take on a popcorn-like structure. A CV of plating solution with chlorophyllin and without chlorophyllin shows that chlorophyllin increases the resistivity of the solution significantly. Because of the small concentrations of chlorophyllin added to achieve this effect, it is likely that the resistance effect occurs at the electrode surface rather than due to lowering the conductivity of the electrolyte itself. In FIG. **5** below, the figure on the left shows a high acid copper solution without the addition of chlorophyllin. The second graph on the right of FIG. **5** shows the same high acid copper solution with chlorophyllin. In FIG. **5**, the top line refers to copper plating and the bottom line refers to copper dissolution. A close examination of the CV shows that the two initial peaks in the forward sweep and reverse sweep occur at the same potentials. However, in the forward sweep of the electrolyte with chlorophyllin, the peak oxidation of copper into ionic form is suppressed, and the final peak occurs at a potential that is 0.3 volts higher than in the solution without the additive. This shows that some another process is occurring at the anode during reduction of copper. This likely occurs due to adhered chlorophyllin desorbing off the surface of the electrodes as potential increased. Furthermore, the peak plating current is also lower in the solution with chlorophyllin, giving support to the idea that chlorophyllin increases the resistivity of the system by preventing the flow of ions.

[0059] In an embodiment represented by this example, copper chlorophyllin is found to have a considerable effect upon the structure of the copper crystals. Chlorophyllin undergoes anodic attraction during alternating pulses, creating a situation in which the chlorophyllin coats the developing dendritic fractal structure, creating regions of even higher thermodynamic instability allowing additional growth of dendrites on the already complex surface. FIG. **6** shows an anodic pulse, and the resulting chlorophyllin film coating the copper electrode.

[0060] The chlorophyllin can produce this effect because it is selectively pulled from the fractal structure in a way that exposes surfaces to rough, protruding points which promote additional dendritic growth. Based on the electrochemistry of chlorophyllin, and its effect on the electrodeposition of copper, proper surface areas can be determined on which reactions can occur. Copper nanostructures are resolved down to length scales as low as 10 nanometers, nearly a full order of magnitude smaller than those previously reported in the literature. FIG. **7** and FIG. **8** show a highly structured dendritic copper particle resolved to 500 nm. These particles have much higher complexities than other particles reported in the literature, and most likely form due to the interaction of the process with copper chlorophyllin. FIG. **9** and FIG. **10** show the result of dendritic agglomeration after 500 pulses and 1000 pulses.

[0061] The result of high current densities running through the relatively low number of nucleating particles results in higher formation of hydrogen bubbles, since the potentiostat is set, in this embodiment, to deliver a constant current rather than a constant potential. Thus the total current is distributed over a much smaller surface area. While dendrites still formed at current densities insufficient to produce hydrogen, hydrogen bubbles serve as a template for the formation or micropores as well as the protrution of dendrites into the micropores. Because the interface of gas and liquid in bubbles form thin channels of liquid, the growth of copper becomes diffusion limited, creating dendritic structures of varying crystal structures. Furthermore, this dendritic pore forms a single, conductive crystal, with the potential to vibrate and transmit phonons through its structure. FIG. **11** shows the incipient formation of copper PDS after 2000 pulses. FIG. **12** shows the final copper PDS grown on glass carbon. The diameter of the pore is about 2 mm and it protrudes about 1 mm off the surface of the glass carbon. FIG. **13** shows close-ups of the fully formed copper PDS, which take the form of buds, leaves, stalks and stems. The space between pore openings are filled with dendritic copper, structured down to only a few nanometers, as shown in FIG. **14**. The outside surface of PDS can be further controlled based on, for example, a program of finishing pulses.

Surface Area Results

[0062] Multiple BET surface areas are taken. While not being bound by any particular theory, it is believed that due to the high reactivity of the copper dendritic powder with air, measurements varied from 19.2 meters square per gram to 41.2 meters squared per gram. Weighing errors are also likely due to the small amount of dendritic powder available to be weighed. However, the median measurement is 29.45, and this corresponds well to 20 meters square per gram previously reported as the BET measurement of a copper tin foam alloy grown under similar conditions, and due to the hydrogen bubble templating. See Shin, H, M. Liu, Copper-Tin electrodes for lithium batteries," Adv. Functional Materials 15, No 4, April (2008). The increased surface area can be due to the dendritic structures protruding from the pores—structures which the Cu—Sn alloy does not possess.

[0063] A <150 micron copper powder (Alrich 99.999% pure <150 micron powder) is tested, a surface area of 1.28 is obtained. However with the fractal powder a BET surface area of 4.26 is obtained despite the visibly larger particle sizes. When the structure is held intact on a piece of glassy carbon, the BET surface area is almost 1 order of magnitude higher, with readings ranging between 19.5 m^2/gram and 41.2 m^2/gram. The high range in the results could be due to errors in degassing the samples. Because of the low stability of the samples used in this Example, degassing at temperatures above 150° C. caused the sample to fall apart, constrict, or otherwise disappear. Thus, degassing is conducted at a relatively low temperature and not all gas can have been equally driven away from the samples. However, this error would tend to bias measurements downwards rather than upwards since sample absorptiveness and sample mass will be underestimated.

TABLE 1

Sample Mass v. BET Measurement

Sample Mass	BET Measurement
0.0055	19.5
0.0022	26.3
0.0032	31.99
0.0052	41.2
0.003	22.4
Average	28.278

[0064] Interestingly, a comparison of BET surface measurements gives insight into the different surface areas of powders. Using 2 grams of copper powder, <150 microns in diameter, this powder has a surface area of only 1.14 meters squared per gram. Even this is a high reading, as there exist reports of copper powders with surface areas as low as 0.5 meters squared per gram. Even dendritic powder grown under high current densities showed a surface area of 4.15 meters squared per gram. Thus, the dendritic structures themselves, as well as the arrangement of the dendritic metals into a foam, both contribute to the increased absorptivity of the dendritic foam. This lends further support to the unique and positive geometries of the dendritic microporous foam, along with the combination of dendritic structures and micropores, both contributing to the gas absorption capabilities of the foam.

[0065] The average pore size of the foam in this example is 10 to 50 microns, which is consistent with those reported in the literature. In certain embodiments that employ higher system pressures, pore sizes can be reduced through the reduction in bubble size of template hydrogen gas. While not being bound by any particular theory, it is believed that the tips of dendrites could be resolved to 50 nanometers, and display a highly textured surface which is also self-similar across multiple scales.

[0066] The high surface area, as well as the electrical conductivity of this material, are noteworthy. The use of these structures in the reduction of CO_2 to ethylene, methane, and/or other hydrocarbons electrolytically, at room temperatures, with nothing more than a saturated solution of carbon dioxide and sodium bicarbonate, can be a highly economic means of producing natural gas from carbon dioxide.

Applications for CO_2 to Liquid Fuels:

[0067] Direct electrochemical reduction of CO_2 allows for a simpler process and also, by avoiding high temperature and pressure reactors, also provides the process production rates to take advantage of baseload surplus electricity (Gatrell 2008). Because of the high absorptivity of these structures, the absorptive resins, in one particular embodiment, are to be used in an electrolytic cell, optionally functionalized onto the copper, to produce a direct means electrolytic reduction of CO_2 to ethylene, methane and/or other hydrocarbons on the surface of the resin support.

[0068] Copper and platinum display catalytic activity on various toxic and undesirable substances, pollutants, residues, and greenhouse gases. Copper is a particularly good catalyst because of its relative low cost, as well as its proven applications in the breakdown and detoxification of organic compounds. High surface area copper can provide rapid decomposition and neutralization of toxins such as hydrazine, trichloroethylene, nitrobenzene, and phenols, as well as the potential for applications in other fields, such as the electrolytic reduction of carbon dioxide to methane, methanol, and other hydrocarbons, and rapid, high current energy generation in fuel cells. Solely for pupose of convenience, this section will discuss the electrolytic reduction of CO_2 on copper electrodes.

[0069] The electrochemical reduction of CO_2 on a Cu electrode has gained attention for the removal and conversion of CO_2 to more useful products, the electrocatalytic activity of Cu electrodes, and the electrode activity as a function of different electrolyte concentrations, temperatures and pressures. See Lee, Jaeyoung, Yongsug Tak: "Electrocatalytic activity of Cu electrode in electroreduction of CO_2; Electrochimica Acta 46 2001 3015-3022; Cabrera, Carlos R., Hector De. Jesus Cardona, and Cynthia del Moral: "Voltammetric study of CO_2 reduction at Cu electrodes under different $KHCO_3$ concentrations, temperatures, and CO_2 Pressures." Journal of Electroanalytical Chemistry 513 (2001) 45-51.

[0070] The creation of porous gas electrodes, which facilitate the conversion of saturated CO_2 to unsaturated CO_2, is one major need in improving the efficiency and commercial feasibility of electrolytic reduction of carbon dioxide to ethylene, methane, methanol as well as formic acid and other hydrocarbons. It is hypothesized by Gattrell et al (2006) that the reduction of CO_2 to CH_4 occurs not from dissolved CO_2 but from gas phase CO_2, due to adsorbed CO_2 on the surface of the electrode, as well as the adsorption of CH_4 and higher hydrocarbons on the surface of the gas electrode. The first reaction is $CO_2+e- \rightarrow CO_{2ads}^-$. For many other catalysts which have high CO adsorption, the production of CO is favored. CO+ both physisorbs and chemisorbs onto copper and is enhanced by surface defects and can form temporary carbonate structures with the copper.

[0071] The reactions involved for the electrolytic reduction of CO_2 to higher chain hydrocarbons are given below; all reactions are given vs. Standard Calomel Electrode. (Collin and Sauvage 1989):

$$CO_2+2H^++2e^- \rightarrow CO+2H_2O \quad E^{o'}=-0.52 \text{ V.}$$

$$CO_2+2H^++2e^- \rightarrow HCOOH \quad E^{o'}=-0.61 \text{ V.}$$

$$CO_2+8H^++8e^- \rightarrow HCHO+H_2O \quad E^{o'}=-0.48 \text{ V.}$$

$$CO_2+8H^++8e^- \rightarrow CH_3OH+H_2O \quad E^{o'}=-0.38 \text{ V.}$$

$$CO_2+8H^++8e^- \rightarrow CH_4+2H_2O \quad E^{o'}=-0.24 \text{ V.}$$

[0072] A rough calculation of the cost of methane can be calculated. A high current efficiency of 60% hydrocarbons,

with the balance being hydrogen, formate, and CO can be achieved using a simple copper foil. Under complete conversion of CO_2 to methane, one would obtain 44 grams CO_2 per 16 grams of methane. The price of 1 mmBTU of natural gas is $4.304 (www.nymex.com). There are 97 cubic feet in 100000 BTU of natural gas and thus there are 970 cubic feet in 1 mmBTU of natural gas. This converts to 27467.341 liters. Using the ideal gas law, PV=nRT, the number of moles of methane can be determined. Thus, there are 1225.49 moles in 1 mmBTU of natural gas. Which will require the same amount of moles of carbon dioxide to produce, Assuming the cost of carbon dioxide is $100/ton and 1 ton is 1000 kg, 1 ton of CO_2 would produce 1000000 g/53922 g=18.5453 mmBTUs of natural gas. Thus, based on the raw material cost of carbon dioxide, the market value of the product would be 18.5453*4.304=$79.82. With a carbon offset price of $35 per ton of CO_2 it is conceivable that natural gas can be produced from CO_2 profitably if the cost of baseload electricity would be negligible in this process. This also assumes a 60% efficiency with other valuable products which produce, neglected in the analysis, 1 mol of CO_2 would require 8 mols of electrons or 13.33 coulombs of energy. Assuming 1 cent per kilowatt hour, it would cost 13.33 cents per kilomol of CO_2 produced, since each mole of CO_2 requires 13.33 coulombs of electricity operating at 60% efficiency. The minimum current that can be used in the reaction would be on the order of $0.5*10^{-2}$ assuming a resistance of 100 ohms. Based on this number, the minimum power requirements for the reaction to proceed is $100*(0.5*10^{-2})^2$ or 0.0025 watts or 0.0000025 kilowatts. To reduce 1 ton of CO_2 to methane would require 13.33*1225.5*18.55 Columbs. At an amperage of $0.5*10^{-2}$ C/second as the lower bound, 1 ton of CO_2 would require (13.33*1225.5*18.55)/0.005=60606244.7 seconds or 16326 hours. Thus 16326*0.0000025=0.040815 kilowatt hours. Of course one would not expect the reaction to proceed at such low amperages, and one could turn up the reaction rates very significantly and still only incur relatively reasonable electricity costs. The primary costs are CO_2 feed stock, and water.

[0073] Interestingly, a mixture of Fischer Tropsch products of up to C_6 hydrocarbons are produced from CO_2 at room temperature. Carbon chain products are observed for copper electrodes which had been polished under an acid solution. See Shibata, Hirokazu Jacob A. Moulijn and Guido Mul: Enabling Electrocatalytic Fischer-Tropsch Synthesis from carbon dioxide Over Copper-Based Electrodes. Gattrell et al (2007) propose that five cells connected in series would be able to convert 97% of Carbon Dioxide fed into the system producing a final product of hythane. Other studies have been conducted on the effect of copper crystal structure on selectivities (Hori et al 2003) and the effect of alloying other metals to copper (Mho et al 2000).

[0074] Other methods of electrocatalytic conversion of CO_2 involve alternative metals such as TiO_2, Pt, as well as using methanol as an electrolyte instead of water (Centi et al 2007). Higher H^+ concentration increased the yield of hydrocarbons in the reduction of CO_2. The results at different temperatures and $KHCO_3$ concentrations support the idea of the presence of CO as an adsorbed intermediate and the existence of a region of lower pH near the electrode surface, respectively. Different pressures also change the current efficiency and products at the copper electrode. Voltammetric study of CO_2 reduction at Cu electrodes under different $KHCO_3$ concentrations, temperatures and CO_2 pressures (DeJesus-Cardona et al 2002).

[0075] Hori et al (1993) tested the selectivity of various metals for CO production from CO_2 and found that Au>Ag>Cu>Zn>>Cd>Sn>In>Pb>Ti>Hg, though copper is still the best producer of hydrocarbons electrolytically. Mediation with metal porphyrins is also studied and found to be an effective means of electrolytic reduction of CO_2. See, Ogura, Kotaro, Ichiro Yoshida: Electrocatalytic Reduction of CO_2 to Methanol part 9: Mediation with Metal Porphyrins." Journal of Molecular Catalysis, 47 (1998) 51-57, hereby incorporated by reference. Copper chlorophyllin, which will reduce carbon dioxide in air at the same rate as a leaf, is of particular note. Losada et al (1995) used polymer films of polypyrrole cobalt(II) to reduced CO_2 electrolytically.

[0076] While poisoning of catalyst has been reported to occur as a major problem of deposition (Yano et al 2001), Hori et al (2005) determined that the deactivation of copper electrodes are, in reality, due to impurities in the prepared solution which could be eliminated through pretreatment. Bockris discusses the importance of preelectrolysis of electrolyte solutions when studying electrode processes in detail (Bockris 1993, Bokris 1970). Catalyst poisoning is not detected on the surface of the catalyst by the CV. The CV shows the current flow as a function of potential. Current is directly proportional to the reduction of CO_2 to CH_4.

[0077] One of the major difficulties with using electrochemical cells for industrial conversion of CO_2 to hydrocarbons is the large geometries necessary for foil electrodes to produce industrial quantities. These structures are especially useful for electrocatalytic application which require high interfacial surface areas or high absorptions of gas reactant species. The extraordinarily high activity potential of the presently disclosed copper chlorophyllin catalyst is due to the high surface area of the dendritic structures as well as the micropores and nanopores in the scaling, self-similar structure, which allows for rapid absorption of reactant species. These structures absorb a notable amount of gas, as determined by a BET test.

[0078] Aqueous electroreduction of CO_2 to ethylene, methane and other hydrocarbons could be a significant strategy for upgrading the value of CO_2 to enhance the economic feasibility of air capture and other CCS (carbon capture and storage) technologies. This is particularly true with ionic resin exchange membranes which capture CO_2, as the technology requires the immersion of the CO_2 saturated membranes into water to facilitate the desorption of CO_2. During the desorption process, the resulting solution can be saturated with CO_2 and fed into an electrolytic cell for the conversion of the gas into hydrocarbons. This could be facilitated with copper dendritic gas diffusion electrodes, which would allow for a high efficiency conversion with the minimal use of copper, a catalyst that is already cheap and plentiful.

[0079] Furthermore, Fisher-Tropsch (FT) synthesis can also be conducted from the higher hydrocarbons produced from the initial copper electrodes. Fisher Trospch synthesis can also be conducted electrolytically at room temperature. The limiting factor again is the solubility of the gas in the electrolyte, as well as the ability of electrodes to adhere gaseous reactant species.

[0080] Through the use of double templating, copper dendrites can be converted to metals thermodynamically preferred, such as gold, silver, and platinum. Furthermore, by producing zinc dendrites, electrolytically, a similar process

can be used to produce iron and cobalt dendritic electrodes which produce similar gaseous effects. Table 2 below gives the reduction potentials of important electrolytic reduction reaction which can be utilized with double templating to produce gaseous electrodes with high efficiencies.

TABLE 2

Standard Potentials. Source: Handbook of Chemistry and Physics, 86th Edition.

Half-reaction	E° (V)
Zn2+ + 2 Zn(Hg)	−0.7628
Zn2+ + 2 Zn(s)	−0.7618
Cr3+ + 3 Cr(s)	−0.74
Fe2+ + 2 Fe(s)	−0.44
C2OO2(g) + 2 + + 2 HOOCCOOH(aq)	−0.43
Cr3+ + e− Cr2+	−0.42
Cd2+ + 2 Cd(s)	−0.40
Cu2O(s) + H2O + 2 2 u(s) + 2OH−	−0.360
Co^{2+} + 2 ==> Co(s)	−0.28
Ni^{2+} + 2 ==> Ni(s)	−0.25
Pb^{2+} + 2 ==> Pb(s)	−0.13
$2CO_2(g) + 2H^+ + 2$ ==>HCOOH(aq)	−0.11
2HCOOH(aq) + 2 + + 2 ==>HCHO(aq) + H_2O	−0.03
2 + + 2 ==>$H_2(g)$	0.0000
C(s) + 4 + + 4 ==>$CH_4(g)$	+0.13
2HCHO(aq) + 2 + + 2 ==>$CH_3OH(aq)$	+0.13
Re^{3+} + 3 ==>Re(s)	+0.300
Cu^{2+} + 2 ==> Cu(s)	+0.340
$Cu^+ + e^-$ ==> Cu(s)	+0.520
2CO(g) + 2 + + 2 ==>C(s) + H_2O	+0.52
I^{3-} + 2 ==> 3	+0.53
$I_2(s)$ + 2 ==> 2	+0.54
$PtCl_4^{2-}$ + 2 ==>Pt(s) + 4 l−	+0.758
$Ag^+ + e^-$ ==> Ag(s)	+0.7996
Pd^{2+} + 2 ==> Pd(s)	+0.915
Au $[AuCl_4]^-$ + 3 ==> Au(s) + 4 l−	+0.93
Au [AuBr2]− + e− ==>Au(s) + 2 −	+0.96
Au [AuCl2]− + e− ==>Au(s) + 2 l−	+1.15
Au^{3+} + 3 ==>Au(s)	+1.52
$Au^+ + e^-$ ==> Au(s)	+1.83

[0081] Any metal with a more positive electromotive potential can undergo electroless plating, in which metal ions which have a higher EMF will spontaneously exchange ions with the metal of a lower EMF. Thus, from the porous copper structure, platinum, silver, palladium and gold can be plated electrolessly to form dendritic pores of a similar structure. Furthermore, if zinc leaves are grown instead of copper leaves, a larger array of potential porous dendritic electrodes could be produced from a wide variety of metals, since zinc has a relatively low EMF. Thus, an electroless process could be used to replace zinc with chromium, iron, nickel or cobalt, all of which can play significant roles in Fischer Tropsch synthesis.

[0082] A further application of the presently disclosed subject matter is the use of carbon nanotubes as electrodes for the further refining of hydrocarbons into FT synthetic fuels. Since the experiments performed are conducted on glassy carbon, a relatively low surface area substrate with a low conductivity and activity (Rozwadowskp 1979), improvements in current efficiencies for reduction of carbon dioxide can be obtained if glassy carbon substrates are replaced with a carbon nanotube substrate as a heterogeneous catalyst support due to the increased absorptive, conductance, and electrochemical activity of nanotubes (Planeix 1994). Many uses of nanostructured electrodes have already been found for electrolytic applications (Wang 2004) for such applications as sensors (Pietrobon et al 2009, Welch et al 2006), fuel cells (Lien et at 2005), and fuel conversion (Tong 2007) and reforming of methane (Pawelec 2006). Direct plating of metal catalyst particles has found some success, though chemical means have been the dominant method of electrode preparation (Yao et al 2004, Yang et al 2009). Nanotubes are already a promising route for high pressure and temperature FT synthesis (Prinsloo et al 2002, Serp et al 2003), including the direct impregnation of high activity catalysts such as cobalt (Choi et al 2002) onto carbon nanotube structures, which has been shown to increase yields of lighter hydrocarbons and lower the peak temperatures of the reaction (Tavasoli et al 2008, Lu 2007) as well as selectivities of specific hydrocarbons (Lordi et al 2001). A combination of the capacity of nanotubes to adsorb and store hydrogen (Mishra et al 2008), as well as its demonstrated high electrochemical activity when decorated with noble and near noble metals (Sun et al 2005, Tang et al 2004, Li et al 2004, Tsai et al 2007, Georgakilas et al 2007) along with the ability of porous copper dendrite to adsorb carbon dioxide and hydrocarbons, make the combination of the two particularly interesting for reduction of CO_2 as well as FT synthesis. No studies on CNT electrolytic reduction of CO_2 have been reported in the literature.

Means of Producing Shape Controlled Nanoparticles:

[0083] This section will review electrochemical mechanisms of producing fractals and dendrites as well as other shape-controlled nanoparticles. It will first discuss electrodeposition and some of the dendritic structures produced with this process. It will then discuss sonochemistry and sonoelectrochemistry as another means of producing fractal nanostructures. Finally, the mechanisms of fractal formation for copper is briefly discussed.

[0084] Electrodeposition:

[0085] Electrodeposition has found application for creating nanostructures with unique properties. Electrodeposition provides a high degree of control and repeatability for production of nanoparticles, including shape control as well as size control, depending upon the applied currents and potentials, as well as nucleation characteristics of electrode materials. See Liu, H. F. Favier, K Ng, M P Zach, and R M Penner: "Size Selective Electrodeposition of Meso-scale Metal Particles: a general method." Electrochimica Acta 47 (2001) 671-677; Radisic, Aleksandar Philippe M. Vereecken, James B. Hannon, Peter C. Searson, and Frances M. Ross: "Quantifying Electrochemical Nucleation and Growth of Nanoscale Clusters Using Real-Time Kinetic Data, Nanoletters (2006) Vol, 6 No 2. 238-242.

[0086] Furthermore, this technique is well understood, and is both economical and fast. Finally, the product of electrodeposition can be harvested directly from electrodes rather than slowly separated out of a mixture, which is often the case in the production of nanoparticles through chemical means. Electrodeposition has been used to produce nanowires directly on carbon nanotubes. Electrodeposition goes a long way towards solving the problem most nanoparticles face: the lack of stability that other methods such as chemical reduction as well as the method of microwave irradiation which are more difficult to structure into a stable, repeatable configurations. Particles can be deposited directly onto a supporting structure such as nanotubes. Catalytic metals relevant to FT

synthesis can be deposited unto carbon nanotubes and other carbon substrates such as glassy carbon as supports include platinum and platinum-ruthenium, gold and silver. See, e.g., Auer E, Freund A, Pietsch J, Tacke T: Carbons as Supports for Industrial Precious Metal Catalysts. Appl Catal A. 1998; 173: 259-71.

[0087] Sonoelectrochemistry:

[0088] Sonoelectrochemistry has also been used to produce fractal and dendritic nanostructures. In order to understand this method, Sonochemistry must first be discussed, and involves using an ultrasonic horn to agitate liquid systems. Sonochemical effects occur because of acoustic cavitation which form as the peaks and troughs of an ultrasonic wave pass rapidly through the liquid medium creating regions of rarification and attenuation, See Adewuyi, Yusuf G: "Sonochemistry: Environmental Science and Engineering Applications." Ind Eng. Chem. Res. 2001 40(22), 4681-4715 DOT 10.1021/ie0100961; Mason, Timothy J., "Large Scale Sonochemical Processing: Aspiration and Actuality." Ultrasonics Sonochemistry 7 (2000) 145-149. This causes formation of bubbles, which are then caused to implode by the moving pressure wave of sound. This results in two regions of enhanced chemical activity: in the gas within the bubbles which reach temperatures of up to 5200 K, and along the boundary between the water and the gas phase, which can reach temperatures of 1900K. Hydrodynamic models of cavitation also estimate pressures of reach betwen 1000-10000 bars. See Suslick, Kennth S. Taeghwan Hyeon, and Mingming Fang: "Nanostructured Materials Generated by High-Intensity Ultrasound: Sonochemical Synthesis and Catalytic Studies." Chem. Material. 1996 8, 2172-2179. (Suslick et al 1986).

[0089] Sonochemistry has been used to produce iron oxide nanoparticles when they are ligands of organic particles. These iron nanoparticles of 20 nm clusters of 2-3 nm smaller subcomponents displayed kinetics of up to 10 times higher than the bulk form. Furthermore, this method is also reported to improve iron selectivity when loaded onto a silica substrate through sonification. Sonification also produces OH radicals which explains many of its effects in the environmental engineering practices, such as phytocatalysis of pollutants. However, the also gives it potential for functionalizing the surface of carbon nanotubes as well as the surfaces of electrodes and catalyst supports for catalyzing reactions such as methanation. See Tong, Hao, Hu Lin Li, Xiao Gang Zhang: Ultrasonic Synthesis of Highly Dispersed Pt Nanoparticles Supported on MWCNTs and Their Electrocatalytic Activity Towards Methanol Oxidation. Carbon 45 (2007) 2424-2432.

[0090] Sonoelectrochemistry couples the power ultrasound to electrochemistry. Kinetics and cavitation are the two main avenues through which sonoelectrochemistry produce its unique results on the nanoscale. Microjets are generated at the electrode surface by the cavitation events with speeds of up to 100 msec. The setup should include an ultrasonic immersion horn probe in which the horn tip can be placed inside the electrochemical cell, producing a sonoelectrochemical cell. The other components would be a graphite counter electrode, Ar inlet degassing unit, Pyrex reservoir to maintain thermal conditions, a Titanium tipped sonic horn, an SCE reference electrode, and Pt 102 resistance thermocouple. A thorough review of the setup can be found in Compton Richard G, John C. Eklund, Frank Marken, Thomas O Rebbitt, Richard P. Akkermans and David N. Waller. "Dual Activation: Coupling Ultrasound to Electrochemistry—An Overview." Electrochimica Acta Vol 42 No 18 pp 2919-2927, which is hereby incorporated by reference.

[0091] According to the literature, sonication enhances current densities of the electrochemical system. Even uncontrolled electrode geometries placed in an ultrasonic bath, enhancing currents to 10 times high than unsonicated electrodes. On glassy carbon electrode surfaces, significant pitting is observed. However, activation of the carbon is also observed, and is theorized to arise from OH— radicals produced in the cavitation bubble, which then react with the surface of the glassy carbon electrode. This activation is not likely due to increased BET surface area. OH— fictionalization of glassy electrodes led to higher rates of electrodeposition of PbO_2. Other aspects which can be controlled are the frequency and intensity, pulsing intervals and lengths, gases in dissolved in solution, pressure and temperature, concentration of solute, and geometry and location of sonic sources. The enhanced reactions spurred by sonoelectrochemical practices are due to a thinning of the diffusion layer between the electrolyte and electrode. Sonoelectrification of CNTs with SbSI has been used to prepare nanorods with the CNT matrix and Co/Fe alloys are also produced with this method. Nowak et al (2009) in their study use the high pressures and temperatures formed by the cavitation bubbles to form nanorods within the CNTs.

[0092] Additives such as PVA have been used in the sonochemical process to prevent the agglomeration of particles as they are deposited. Hass et al (2008) used a sonoelectrochemical method to synthesize copper dendrite nanostructures. See Haas, Iris, Sangaraju Shanmugam, and Aharon Gedanken, "Synthesis of Copper Dendrite Nanostructures by a Sonoelectrochemical Method." Chem. Eur. J. 2008, 14, 4696-4703. Because sonochemistry relies on ultrasonic pulses that produce small bubbles which collapse very quickly (Compton 1997), this can explain why dendritic structures form. Lead Oxide nanostructures are created using ultrasonic pulses on a glassy carbon electrode (Garcia et al 1998). It is likely that these dendritic structures form as a powder, which are later linked together on the carbon matrix by the intereaction between the polymer chains which hold the particles together and prevent them from agglomerating, as well as the interaction between the PVA and the carbon matrix. PVA functions by forming a polymer matrix which creates this effect, while the —OH group allows for electric interaction between particles, which would be prevented from occurring by the surfactant PVP. They concluded that neither the electrode, nor the pulseform or pretreatment made any difference in the dendritic structures formed, and instead these formed only after on the carbon-copper matrix used in TEM studies. Haas reported that the BET surface area of the dendritic structure is less than 2 m^2/gram.

[0093] Haas does not explain the mechanism of dendrite and fractal formation beyond suggesting the electronic interaction. However, given the results of the formation of copper dendrite foam, it seems likely that dendritic powder formation occurs due to the same mechanism, whereby bubble formation create diffusion limited conditions which promote the formation of dendritic structures. Their method is interesting in that they have a 300 ms pulse of electricity followed by a 250 ultrasonic pulse. The electric pulse causes the copper to be reduced into a polymer matrix formed on the PVA, which is then ablated off the electrode by the ultrasonic pulse. Then searching for the deposition of dendritic fractal struc-

tures which had dimensions between 1.74 and 1.76, and had details of up to 50 nm in resolution, these dendrites are dependent upon the interaction between the colloid solution and the interface on which it is prepared to be scanned rather than from any inherent activity from the sonoelectrochemical cell. The major contribution of the sonoelectrochemical cell is to create nanoparticles from reduction of copper, and then the stabilization of these nanoparticles by the PVA. Intriguingly, the dendritic structures only formed on a copper carbon grid, which is used as preparation material for TEM study. Perhaps, by creating a electrical matrix on the surface of carbon nanotubes, it can be possible to load nanotubes with dendrites. The use of surfactants has also been reported to create tin nanorods in conjunction with a sonochemical method (Qiu et al 2005). Dendritic crystal growth occurs in electrochemical conditions far from thermodynamic equilibrium. Dendrites tend to grow under mass transport limited conditions. At conditions far from thermodynamic equilibrium, surface energy is no longer the dominant factor in crystal formation (Choi, Kyoung-shin 2008).

Dendrite Formation:

[0094] Dendrites are also the most efficient way to distribute surface area in a three dimensional structure while maintaining a coherent, single structure. Other dispersion methods optimize the total catalytic surface area, without maintaining a coherent shape that also preserves the charge transport properties of the metal. While interest in the formation of non-noble nanoparticles and structures have been growing due to the relatively high stability of copper nanoparticles, the presently disclosed subject matter relates to uses of porous copper dendritic structures. One advance in copper dendritic structures has come where the porous dendritic structures grown under high current densities can be used as a template to electrolessly exchange copper ions with platinum ions, creating a dendritic structure that is fully platinum. These structures have been shown to increase the current density of the electrocatalytic reduction of O_2 over 2.5 times.

[0095] This section will discuss crystal growth in copper and the conditions necessary for dendrite formation to occur. High ionic concentrations will not necessarily affect the crystal growth rate, as the current applied determines the amount of a substance deposited. However, the concentration will affect whether deposition occurs in a mass transport limited regime. The literature suggests that branching growth even at low overpotentials result from an uneven distribution of potential across the surface of the crystal structure. The reduction of Cu^{2+} to Cu^{+} depends on the concentration of Cu^{2+} as the Nernst equation shows:

$$E_{red}=E^{o}-0.05916\times\log([Cu^{+}]/[Cu^{2+}] \text{ at } T=298.15 \text{ K.} \quad 11)$$

[0096] This mechanism can be used to produce dendrites at low overpotentials in low ion concentrations. Different crystal growth regimes can be established depending on the over potential. The growth rate of crystals depends upon the overpotential applied to the electrochemical system. The overpotential, is defined as $N=|E_{appl}-E_{red}|$. The higher the overpotential, the further the system is from equilibrium.

[0097] Mass transport is the most important factor in dendritic crystal growth. Mass transport-limited growth occurs when the rate of crystal growth is greater than the availability of ions in the immediate mass transport boundary layer. Imperfections in the crystal faces create a nonlinear effect in these conditions, as the apexes of the imperfections grow at a higher rate than the receded faces, further increasing the differences between the apexes and valleys of the crystal faces. At high overpotentials in relatively low concentrations of metal ions, a diffusion boundary layer forms around the electrode, which leads the deposition into a mass transport limited regime. High overpotentials also increase the number of crystal branches as well as the total surface area per volume.

[0098] Some factors will prevent the system from reaching a diffusion limited regime. At high concentrations of metal ions, the transport regime cannot become diffusion limited. Higher temperatures also tend to increase the size of the boundary layer and mitigate the depletion zone, thus leading the system to remain outside the diffusion limited regime for higher overpotentials. This is true in the growth of zinc crystals as discussed in the literature. At higher temperatures, the rate of mass transport and the rate of diffusion across the boundary layer increase. Finally, any other factors which tend to contribute to mass transfer, such as stirring rates or short plating pulses would also mitigate the growth of dendrites. Furthermore, capping protruding edges would also tend to reduce the formation of dendrites, by directing crystal growth toward non-dendritic protrusions on the electrode.

[0099] The effect of organic additives on dendrite growth has been studied. One means to study the interaction of additives and crystal growth is to introduce additives into the plating solution after initial growth has already occurred. This allows for the study of crystal faces which might have otherwise been dissolved by the additive. Additives change crystal structure primarily by changing the kinetics and thermodynamics of crystal growth. PVP has been used to prevent the growth of dendrites (Haas 2006) by capping the protruding nucleations. PVP is attracted to the cathode, and is a non polar capping agent, preventing electric interaction between ions and nucleated metals. PEG and PVA on the other hand, do not necessarily promote the growth of dendrites, but change the morphology of the deposits. Finally, chlorophillin is an interesting substance because it both contains a copper core, while also displaying anodic attraction. No studies have been conducted on chlorophyllin to date, as known to the inventors.

[0100] Choi, Kyoung-Shin (2008) discusses shape control through electrodeposition and the use of additives. Different crystal planes have different chemical and physical properties. Furthermore, control of branch growth also changes the distribution of crystals and the connectivity which can play a critical role in the optimization of surface structure. Surfactants such as sodium dodecyl sulfate absorbs to the {111} crystal plane, which slows the growth of branch structures, as the {111} plane is the furthest protruding plane. On the other hand Cl– interact with the {100} direction, resulting in retardation of growth along this axis. The degree of hinderance depends upon the concentration of additives. Initially it is thought that pH is the dominant influence in shape evolution, though later studies showed that the Cl– ion is the determining factor (Choi, Kyoung-Shin (2008)).

[0101] There have only been a few studies published about the control of copper morphology on the nano and micro scales. Dendrites tend to grow under mass transport limited conditions, far from thermodynamic equilibrium where surface energy is no longer the dominant factor in crystal formation (Choi 2008). Imperfections in the crystal faces creates a nonlinear effect in these conditions, as the apexes of the imperfections grow at a higher rate than the receded faces, further increasing the differences between the apexes and

valleys of the crystal faces. Furthermore, as reported by Nikolic et al (2009), as well as Shin et al (2003), when mass transfer limited deposition occurs in the hydrogen evolution regime, evolving hydrogen bubbles form a template around which copper dendrites can form. Manipulating the pause-to-pulse ratio gives greater control over the size of micropores, while variation on voltages can give some control over the morphology of the dendrites (Nikolic 2007). The resulting foam maintains its structural integrity, unlike other dendritic deposits. When grown without additives, Shin reported copper is structured down to hundreds of nanometers. Nikolic et al (2006) reports that the size of the copper grains decrease with increasing over potentials of 550 mV to 1000 mV. A similar copper-tin foam structure is characterized using BET surface measurements to have 20 m^2/gram (Shin and Liu 2005).

[0102] Dendrites form a tree-like structure with a backbone as well as leaves. The physical connection between the crystals of the leaves as well as the backbone crystal allow nanocrystals to act as a single crystal, conducting phonons and electrons as a single structure (Choi 2008). The continuous structure of metallic dendritic structures can provide the first clue as to novel catalyst actions as will be further sketched out in this thesis. Porous dendritic structures occur because of mass transport limited branching growth. The hydrogen bubbles evolved during electrodeposition of copper at high potentials results in the formation of diffusion limited regions near the cathode. These diffusion limited regions produce branching structures while the bubbles create a template for the development of porous dendritic structures.

Theory and Models of Fractal Geometry

[0103] Recently, Copper PDS have been synthesized from copper, as well as other metals such as tin, to form metallic foam with high surface area and high adsorptive characteristics. Many experts in catalysis dismiss the notion of dendritic surfaces as being economically viable for applications due to the assumed short lifetimes of their surfaces. While fractal distributions of catalytic metals have been proposed, only a few multi-scale structures which display self similarity have been synthesized. Furthermore, these structures are usually too delicate to find practical use. However, copper PDS have a higher stability than other fractal distributed catalysts grown at the submicron scale, as these dendritic structures are structured on both a microscale and macroscale and form a continuous structure, rather than a powder. Anecdotal observations of the structure recorded an ability to resist oxidation while maintaining cohesion within an aqueous environment. These structures are completely metallic and display surface areas which are orders of magnitudes higher than metals in their bulk form. Their shape follow fractal geometries, which display self-similarity across multiple scales, and surfaces which grow with the complexity of the surface roughness. PDS have the potential to capture the theoretical effects of fractal surfaces. Studies have demonstrated that catalytic metals arranged in a fractal geometry show higher kinetic rates at lower temperatures.

Review of Fractals and Catalysts.

[0104] Because of the complex interfaces displayed by fractal surfaces, theorists have posited that these surfaces could possess unique applications for catalysis, as well as unique mass and heat transfer properties. Rates of reactions are affected by diffusion effects as well as surface area effects. Geometric effects have also been discussed, and become significant at smaller scales. Catalyst surfaces have been found to have a random fractal, or multi-fractal geometry. Furthermore, catalyst surfaces in simulations have been found to have a significant effect on the rates of reactions of the catalysts, especially those limited by knudsen diffusion, where diffusion occurs along a long pore and collissions occur frequently (Sheintuch 2001). However, these theoretical studies only quantified existing catalyst supports and their conclusions mainly pertained to issues of mass transfer, rather than to the kinetic effect different fractal geometries of metal catalysts themselves might have on catalytic reactions.

[0105] Computer simulations have been conducted in exploring the potential effects of fractal surfaces. Authors have posited that heterogeneous fractal surfaces and fractal pore structures can produce novel effects such as enhanced mass transfer and selectivity. Pfeifer and Avnir (1983) state in their article a power law relating the size of an object R and fractal dimension D to its chemical interaction property.

$A \sim s^{(2-D)/2}$ for monolayer coverage with s=cross sectional area of particles. 1)

$A \sim R^{D-3}$ for adsorbates, where R is the radius of particles 2)

$dV/dp \sim p^{2-D}$ for pores where dV is the infinitesimal pore volume with radius>dp. 3)

[0106] The dendritic porous copper foam would have a combination of contributions from equation 1) and equation 3). These power laws state: that the more complicated the surface, the higher the surface area available for adsorption; and, that the larger the radius and the larger the fractal dimension, the higher the chemical interaction property. Furthermore in Avnir (1991) the catalyst activity is described with another relatively intuitive equation:

$A \sim R^D$ where A is the chemical activity of the particle 4).

[0107] Other studies have made correlations between the activity of a catalyst and its fractal dimension, as a higher fractional dimension implies a more complex surface with more surface area. The justification for this is that porous dendritic structures are controlled fractal surfaces, rather than random fractal surfaces. Meankin's (1986) simulation of catalyst selectivity in random fractals finds small effects due to the unique geometries of random fractals. However, controlled fractal surfaces, can have very specific effects on different types of chemical reactions catalyzed by the base metals beyond those found by Meakin. For example, the porous dendritic structures described in this paper, might have a geometry which deflects gas particles into paths which maximize the number of impacts with the catalyst surface.

Fractal Cage

[0108] The mechanisms simulated are based on the inner recesses of the fractals to have a higher ability to absorb a particle of a specific size, and thus create new products. However, the fundamental mechanism of action would be similar: that though the distribution of catalysis events is equal on all surfaces, the distribution of diffusion absorption events varies greatly as some surfaces are harbored from certain objects (Meakin 1986), perhaps because of their geometry.

[0109] Under certain geometries with involutions, the concentrations of different species of chemicals depending on their molecular mass, would be limited by the depth of scale. It is possible a specific geometry will catalyze a specific reaction to completion very quickly so that production rates are fast which the dominant products produced at one scale, the products reactions occurring on another. There is a multi component recursive product chain of products produced in one of the involutions, as on reactant becomes the reactants on the next. The consumptions of small products, creates a gradient for new monomers to diffuse into the regions, and the random kinetic activity between inflowing monomers will displace new monomers. Certain regions of the fractal surface become inaccessible to diffusion gradients (Meakin 1986). There regions can act as a harbor for creation of a specific type of chemical species.

[0110] One can assume that metals are delocalized electron shells which have the capacity to absorb kinetic energy from surrounding molecules, while also imparting electronic energy to reacting species. If one were to assume that metals, which are high conductors of heat, do not possess kinetic energy when in solid state, then each molecule that strikes the surface of the delocalized shell of an electron will impart some fraction of its energy, 1/f, to metal surface plus a constant, c, amount of energy which is the attractive surface energy of the metal. The reacting species will subsequently slow down. Species which have a low enough kinetic energy below the surface binding energy of the metal will stick to the surface of the metal. When two demobilized reactant molecules come in contact on the surface of the metal, the vibrational energy their reaction creates can be high enough for them to leave the surface of the metal.

[0111] If this is true, then a fractal geometry would be significantly better than another standard Euclidian geometry. Surface area is not the primary determinant of catalyst activity, in itself. Rather, surface area is only important in increasing the number of collisions with reactant molecules. However, an optimized 2 dimensional coating of catalyst particles will still be of a lower efficiency than a porous fractal geometry because fractal geometries maximize the collisions per molecule by directing the trajectory of molecules after the collision towards another metal surface in the vicinity, whose angle directs particles towards another internal wall of the porous dendritic cage. Reactant molecules are trapped within the interfacial spaces and slow down dramatically faster because of multiple collisions. Because of the potential for multiple collisions, even molecules which are moving with initial kinetic energy which exceeds the surface binding energy of the metal, can be demobilized after multiple collisions with the surface of the metal.

[0112] If we assume a flat surface, as is the case with most catalyst loading geometries, then we should assume a fast moving molecule will likely have at most a single collision. Especially if the loading of catalyst particles are only a small percentage of the total surface area on a supporting structure. Since reactant molecules can only have a single collision, their kinetic energy cannot exceed c. However, for multiple collisions, a molecule can have kinetic energy $E^*(1-f)^i$ where i is the total number of collisions for a given molecule and E is the initial kinetic energy of the molecule upon entering the cage. It will also gain energy from collisions with other molecules and collisions with infrared photons emitted by the surface of the metal. However, if the catalyst surface is a polycrystalline with higher heat and phonon conductivity than the surrounding region, and it is connected to an effectively infinite heat sink, the infrared radiation given off by the metallic catalyst surface would likely not exceed ambient temperatures, despite what is an effective hot spot trap within the fractal pore, since the metal can be said to absorb the kinetic energy throughout its delocalized electron shell, and only has average excitation equal to the average kinetic energy it absorbs.

[0113] The pore can become a hotspot because when first exposed to the ambient environment with a given temperature T, which has a corresponding Kinetic energy KE, carried primarily by the movement of molecules. As these molecules come into contact with the opening of the hole, it has a probability p for every unit of time t of getting trapped by the cage. Furthermore, there is a probability q that a particle will escape from the trap where q depends on the number of particles trapped by the cage t with $q<p$. At some point, p and q will equilibrate and the average number of particles per unit volume will be greater within the fractal trap than outside the fractal trap. Furthermore, particles can constantly lose kinetic energy based on each collisions with the surface of the metal, as the metal carries away the energy from particles with higher kinetic energy. Thus, if the average number of collisions for a molecule within some involution of the fractal surface is S, and assuming a uniform distribution of energies. The proportion of molecules which could be captured by a surface with binding energy B would be those molecules which have an energy $E \leqq B$. If we assume a normal Gaussian distribution for the kinetic energy of particles within the system, then the proportion of particles which have an energy less than B for a flat surface would be the cumulative density function of a normal Gaussian distribution where x equal in this case to the normalized number (B−E)/E and the probability of binding would be

$$\Phi(x) = \frac{1}{\sqrt{2\pi}} \int_{-\infty}^{(B-E)/E} e^{-t^2/2}\, dt \qquad 5)$$

[0114] On the other hand, assuming there is a slight loss of kinetic energy by particles in a collision where f is the average proportion of energy lost for each particle after a collision with a metallic surface, while also including energies gained from random collisions with infrared radiation and collisions with other molecules. Assuming that one closes off the opening of the pore system to prevent any new particles from entering, then the new average kinetic energy of the pocket would be

$$E^*(1-f)^i \qquad 6)$$

[0115] Since the average kinetic energy of the system is shifted to a lower energy if one assumes a closed set of particles and a heat sink attached to the metal phonon conductor. Regarding the heat sink, the fractal structure, since it is a continuous structure, will have an increase of kinetic energy transferred through it as phonons, though it does not violate the second law, since these phonons are attached to a glassy carbon surface, which is catalyzed at relatively low temperatures of approximately 200 degrees Celsius.

[0116] The probability of a particle exceeding the binding energy of the metal is:

$$\Phi(x) = \frac{1}{\sqrt{2\pi}} \int_{-\infty}^{(B-E*(1-f)^i)/(E*(1-f)^i)} e^{-t^2/2}\, dt \quad 7)$$

[0117] Finally, the difference between a flat catalyst surface, and a surface which is arranged in a fractal trap would be:

$$\Phi(x) = \frac{1}{\sqrt{2\pi}} \int_{(B-E)/E}^{(B-E*(1-f)^i)/(E*(1-f)^i)} e^{-t^2/2}\, dt \quad 8)$$

[0118] One simulation (Phillips et al 2003) conducted with Fluent CFD using Gambit mesh generator, utilized the Cantor set generator, a 76% reduction in the active surface area, the calculated drop in mass transfer to the active surfaces is only reduced by 2.25% when the reactions are diffusion limited. With each iteration, the total length is shortened by ⅓. However, even after infinite iterations, where the effective length is 0, under this study, the simulations show that the total rate of mass transfer falls asymptotically to a fixed value.

[0119] The present invention is not to be limited in scope by the specific embodiments described herein. Indeed, various modifications of the invention in addition to those described herein will become apparent to those skilled in the art from the foregoing description and the accompanying figures.

[0120] Patents, patent applications, publications, product descriptions, and protocols are cited throughout this application, the disclosures of which are incorporated herein by reference in their entireties for all purpose.

1. An electrolytic cell system to convert carbon dioxide to a hydrocarbon comprising:

(a) a first electrode including a substrate having a metal porous dendritic structure applied thereon;

(b) a second electrode; and

(c) an electrical input adapted for coupling to a source of electricity, for applying a voltage across the first electrode and the second electrode.

2. The electrolytic cell system of claim **1**, wherein the metal is selected from platinum, gold, silver, zinc, cobalt, nickel, tin, palladium and copper.

3. The electrolytic cell system of claim **2**, wherein the metal is copper.

4. The electrolytic cell system of claim **1**, wherein the substrate is selected from copper, copper foil, glassy carbon and titanium.

5. The electrolytic cell system of claim **1**, wherein at least one of the first electrode and the second electrode is at least partially saturated with carbon dioxide.

6. The electrolytic cell system of claim **1**, further comprising an electrolyte source capable of being introduced into a region in between the first electrode and the second electrode of the electrolytic cell system.

7. The electrolytic cell system of claim **6**, wherein the electrolyte is selected from a bicarbonate salt, sodium chloride, carbonic acid, hydrogen, potassium and methanol.

8. The electrolytic cell system of claim **6**, further comprising a membrane to dissolve carbon dioxide in the electrolyte.

9. The electrolytic cell system of claim **5**, further comprising a conduit to pass carbon dioxide directly to the surface of the first electrode.

10. The electrolytic cell system of claim **1**, further comprising a source of a metal porphryrin salt capable of being introduced into a region in between the first electrode and the second electrode of the electrolytic cell system.

11. The electrolytic cell system of claim **10**, wherein the metal porphyrin salt is a metal chlorophyllin salt.

12. The electrolytic cell system of claim **11**, wherein the metal chlorphyllin salt is copper chlorophyllin.

13. An electrode for an electrolytic cell system comprising a substrate with a metal porous dendritic structure applied thereon.

14. The electrode of claim **13**, wherein the metal is selected from platinum, gold, silver, zinc, cobalt, nickel, tin, palladium and copper.

15. The electrode of claim **14**, wherein the metal is copper.

16. A method of converting carbon dioxide to a hydrocarbon comprising:

providing an electrolytic cell that includes

(a) a first electrode including a substrate having a metal porous dendritic structure applied thereon;

(b) a second electrode, and

(c) an electrical input adapted for coupling to a source of electricity, for applying a voltage across the first electrode and the second electrode;

introducing a source of carbon dioxide to the electrolytic cell; and

applying the voltage across the first electrode and the second electrode.

17. The method of claim **16**, wherein the metal is selected from platinum, gold, silver, zinc, cobalt, nickel, tin, palladium and copper.

18. The method of claim **16**, wherein the metal is copper.

19. The method of claim **18**, wherein the copper dendritic structure is prepared by a process that includes adding copper chlorophyllin to the electrolytic cell and electrodepositing the copper chlorophyllin on the first electrode.

20. The method of claim **16**, wherein the carbon dioxide is obtained from an air stream, a combustion exhaust stream, or a pre-existing carbon dioxide source.

21. The method of claim **16**, wherein the hydrocarbon is ethylene.

22. A method for preparing an electrode for use in an electrolytic cell comprising:

(a) providing an electrolytic cell;

(b) applying a solution of a metal porphyrin salt to the electrolytic cell; and

(c) applying electricity to plate the metal porphyrin salt on the substrate.

23. The method of claim **22**, wherein the metal porphyrin salt is a metal chlorphyllin salt.

24. The method of claim **23**, wherein the metal chlorophyllin salt is copper chlorophyllin.

25. The method of claim **22**, wherein the metal porphyrin salt is pulse plated or reverse pulse plated on the substrate.

26. The method of claim **22**, wherein the metal porphyrin salt is applied to the substrate using high current density to create hydrogen bubble templates on the surface of the substrate.

* * * * *